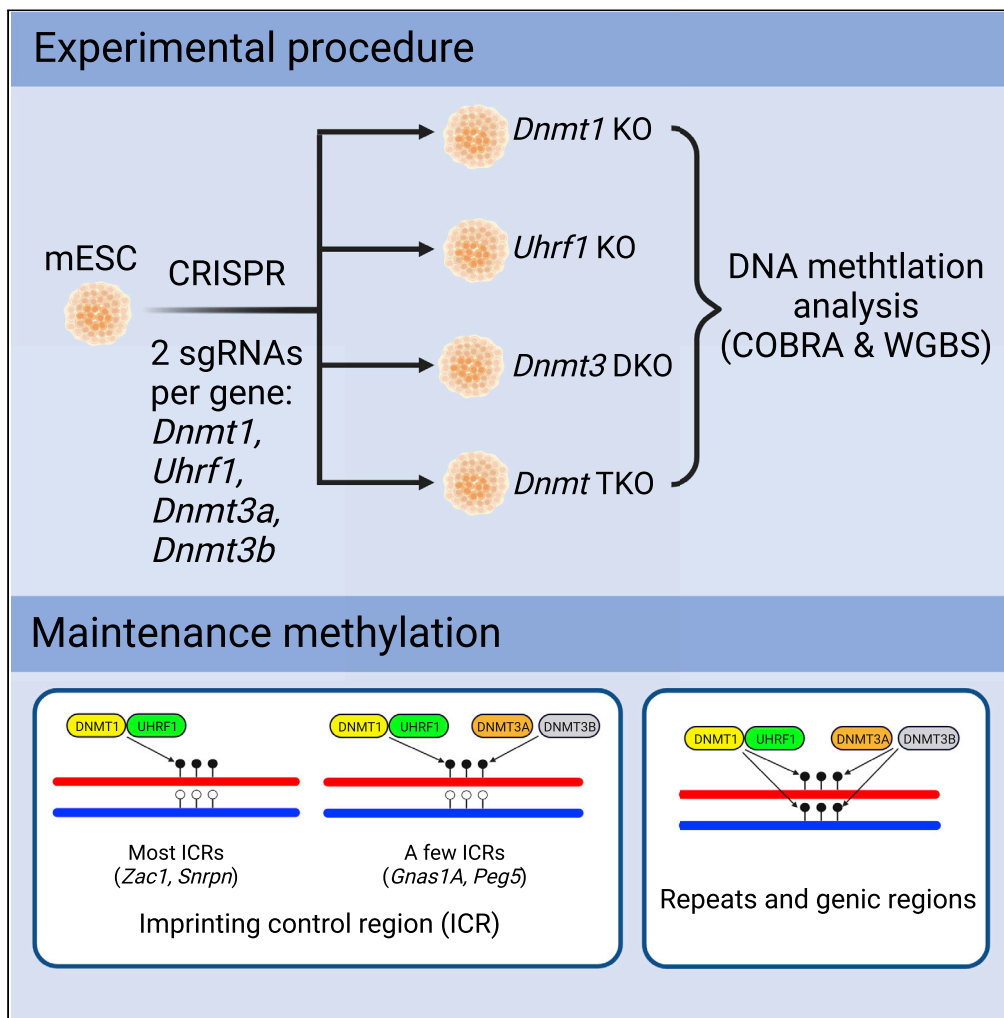**Article**

DNA methyltransferases are complementary in maintaining DNA methylation in embryonic stem cells

Yuhan Liu, Zhen Xu, Jiajia Shi, ..., Wei Xie, Haodong Lin, Xiajun Li

lixj1@shanghaitech.edu.cn

Highlights

ZFP57 maintains DNA methylation at the ICR of most imprinted regions in ES cells

TET proteins may not be essential for maintaining most ICR DNA methylation in ES cells

DNMT3 is required for the maintenance of DNA methylation at a subset of ICRs in ES cells

Maintenance functions of DNMT1 and DNMT3 are complementary at repeats and genic regions

Article

DNA methyltransferases are complementary in maintaining DNA methylation in embryonic stem cells

Yuhan Liu,[1,2,3,8] Zhen Xu,[1,8] Jiajia Shi,[1,8] Yu Zhang,[4,5,8] Shuting Yang,[1,8] Qian Chen,[1] Chenglin Song,[1] Shuhui Geng,[1] Qing Li,[2] Jinsong Li,[2] Guo-Liang Xu,[2] Wei Xie,[4] Haodong Lin,[6] and Xiajun Li[1,7,9,*]

SUMMARY

ZFP57 and ZFP445 maintain genomic imprinting in mouse embryos. We found DNA methylation was lost at most examined imprinting control regions (ICRs) in mouse *Zfp57* mutant ES cells, which could not be prevented by the elimination of three TET proteins. To elucidate methylation maintenance mechanisms, we generated mutant ES clones lacking three major DNA methyltransferases (DNMTs). Intriguingly, DNMT3A and DNMT3B were essential for DNA methylation at a subset of ICRs in mouse ES cells although DNMT1 maintained DNA methylation at most known ICRs. These were similarly observed after extended culture. Germline-derived DNA methylation was lost at the examined ICRs lacking DNMTs according to allelic analysis. Similar to DNMT1, DNMT3A and DNMT3B were required for maintaining DNA methylation at repeats, genic regions, and other genomic sequences. Therefore, three DNA methyltransferases play complementary roles in maintaining DNA methylation in mouse ES cells including DNA methylation at the ICRs primarily mediated through the ZFP57-dependent pathway.

INTRODUCTION

Genomic imprinting is essential for normal development in mammals (Li and Li, 2020; Li et al., 2019a; Li, 2013; Tucci et al., 2019). It is characterized by parent-of-origin-dependent mono-allelic expression of a few hundred imprinted genes (Barlow and Bartolomei, 2014; Bartolomei et al., 2020; Khamlichi and Feil, 2018; Li et al., 2019b). Most of the known imprinted genes are clustered in over 20 imprinted regions in the mouse genome. These clustered imprinted genes are co-regulated by a cis-acting imprinting control region (ICR) in each imprinted region (Barlow and Bartolomei, 2014). Each ICR harbors a germline-derived differentially methylated region (DMR) that modulates the expression of the imprinted genes. Differential DNA methylation at the ICRs is reset in germ cells, with the removal of the original DNA methylation followed by the re-establishment of new DNA methylation at the ICR regions (Barlow and Bartolomei, 2014). The patterns of differential DNA methylation at the ICRs are reconstituted again in the zygote and stably maintained thereafter in the somatic cells of the progeny.

ZFP57 is a KRAB zinc finger protein required for the maintenance of DNA methylation at most known ICRs in mouse embryos (Hirasawa and Feil, 2008; Jiang et al., 2021; Li et al., 2008). Human ZFP57 has similar functions to mouse ZFP57 that it maintains genomic imprinting in humans and it can also substitute for mouse ZFP57 in maintaining DNA methylation imprint in mouse ES cells (Mackay et al., 2008; Takikawa et al., 2013). ZFP57 can recognize the six-nucleotide consensus motif TGCCGC that is present at almost all known ICRs, with a much higher binding affinity for the ICR sequences with methylated DNA (Liu et al., 2012, 2013; Quenneville et al., 2011; Strogantsev et al., 2015). It binds to the cofactor KAP1/TRIM28 via its KRAB box which in turn may recruit DNA methyltransferases to maintain DNA methylation at the ICRs (Li et al., 2008; Quenneville et al., 2011; Zuo et al., 2012). ZFP445 is another KRAB zinc finger protein that has also been shown to regulate genomic imprinting, with more prominent roles in humans than in mice (Juan and Bartolomei, 2019; Takahashi et al., 2019).

Most DNA methylation occurs at the CpG sites in mammals, with a methyl group attached to the fifth position of the cytosine pyrimidine ring (5mC) (Zeng and Chen, 2019). DNA methyltransferases (DNMTs) are the enzymes that catalyze the methylation of cytosine by transferring a methyl group from the donor

S-adenosyl-L-methionine (SAM) (Li and Zhang, 2014). There are three well-known DNMTs in mammals, i.e. DNMT1, DNMT3A, and DNMT3B, with each containing an active DNA methyltransferase catalytic domain (Chen and Zhang, 2020). DNMT3L has sequence homology to these three DNMTs but does not have the active catalytic domain, although it can bind to DNMT3A and DNMT3B to enhance their catalytic activities. Passive loss of DNA methylation may occur during DNA replication if there is no maintenance methylation. Usually DNMT1 is considered to be the maintenance DNMT, whereas DNMT3A and DNMT3B participate in *de novo* methylation. UHRF1 has a functional domain for binding to hemi-methylated DNA and it helps DNMT1 to copy the methylation patterns on the parental strands to the newly synthesized strands after semi-conservative DNA replication (Mancini et al., 2021; Zhang et al., 2019).

Besides replication-dependent passive demethylation, DNA methylation at the CpG sites may be removed through the oxidative demethylation process mediated by Ten-Eleven Translocation (TET) proteins (Wang et al., 2020; Xu and Bochtler, 2020). There are three TET proteins (TET1, TET2, and TET3) in mammals (Wu and Zhang, 2017). TET can convert 5-methyl cytosine (5mC) to 5-hydroxymethyl cytosine (5hmC) first, which can then be further oxidized by TET to give rise to 5-formlycytosine (5fC) and subsequently 5-carboxylcytosine (5caC) (Bochtler et al., 2017). These oxidized cytosine derivatives cannot be recognized by DNMTs and thereby DNA demethylation occurs when they are serially diluted during multiple rounds of DNA replication (Wu and Zhang, 2014). Alternatively, they may be excised by TDG and other DNA repair enzymes through the base excision repair (BER) pathway, which results in DNA demethylation (Hu et al., 2014).

Embryonic stem (ES) cells are pluripotent stem cells that have the potential to give rise to different cell types. Nuclear transfer-derived ES (ntES) cells and induced pluripotent stem (iPS) cells also have multi-potential properties and they are good candidates for cell replacement therapies (Bar and Benvenisty, 2020). However, there are a number of studies indicating that genomic imprinting, including the germline-derived differential DNA methylation at the ICRs, is variably lost in ntES and iPS cells (Bar and Benvenisty, 2019; Li et al., 2019b). As the dysregulation of genomic imprinting causes a number of human diseases including cancer and diabetes, it is critical to examine how it is stably maintained in ES cells (Monk et al., 2019). This may help to derive therapeutically suitable ntES cells and iPS cells in the future with relatively stable DNA methylation at the ICRs.

Mouse ES cells are usually derived from the inner cell mass of the blastocysts. In a previous study, we derived a wild-type 129/DBA hybrid ES cell line called D1911 from the blastocyst derived from the timed mating between a 129S6/SvEvTac female mouse and a DBA/2J male mouse (Lau et al., 2016b). To analyze the functions of ZFP57 and ZFP445 in ES cells, we generated multiple deletion mutant ES clones using a CRISPR-based approach developed in our lab and then examined DNA methylation at the ICRs in the mutant ES cells (Liu et al., 2022). We also obtained multiple deletion mutant ES clones that lack one or two or three DNMTs from D1911 with the same CRISPR approach (Liu et al., 2022). Similarly, we also analyzed DNA methylation at the ICRs and other genomic regions including the somatic DMRs and repeats. We took advantage of SNPs present in the 129/DBA hybrid ES cell line and determined the allelic DNA methylation at the ICRs and DMRs harboring SNPs in these mutant ES cells.

RESULTS

ZFP57 maintained most DNA methylation imprint in mouse embryonic stem cells

The mutant ES clones with deletions at *Zfp57*, *Zfp445*, or both were generated by CRISPR-Cas9 from the parental wild-type (WT) 129/DBA hybrid ES cell line D1911 (Tables S1 and S2) (Figures S1A and S1B) (Lau et al., 2016b; Liu et al., 2022). No wild-type ZFP57 was detected in these *Zfp57* mutant ES clones based on Western blot with affinity-purified rabbit polyclonal antibodies against ZFP57 (Figure S2A) (Li et al., 2008). Genomic DNA samples isolated from these mutant ES clones and the WT control ES cells were subjected to COBRA analysis to examine DNA methylation at the ICRs of some known imprinted regions (Figure 1). We found DNA methylation was lost at the ICRs of the *Snrpn*, *Zac1*, *Peg3*, and *Peg13* in *Zfp57*$^{-/-}$ and *Zfp57*$^{-/-}$; *Zfp445*$^{-/-}$ (DKO) mutant ES clones compared with the WT ES clone (Figure 1). Complete loss of DNA methylation was observed at the IG-DMR of the *Dlk1-Dio3* imprinted region in *Zfp57*$^{-/-}$ mutant ES clones, whereas there was residual DNA methylation at this ICR in *Zfp57*$^{-/-}$; *Zfp445*$^{-/-}$ (DKO) mutant ES clones compared with the WT ES clone (Figure 1). DNA methylation was also partially lost at *Peg1*, *Kcnq1ot1*, *Gpr1*, and *Peg5* ICRs in *Zfp57*$^{-/-}$ and *Zfp57*$^{-/-}$; *Zfp445*$^{-/-}$ (DKO) mutant ES clones compared with the WT ES clone (Figure 1). There was no loss of DNA methylation at these ICRs in *Zfp445*$^{-/-}$ mutant ES clones except for the partial loss of DNA methylation at the *Peg5* ICR in 1 out of 2 *Zfp445*$^{-/-}$ mutant ES clones (Figure 1). DNA methylation remained intact at the *Slc38a4* ICR, but it was largely lost at the *Gnas1A*
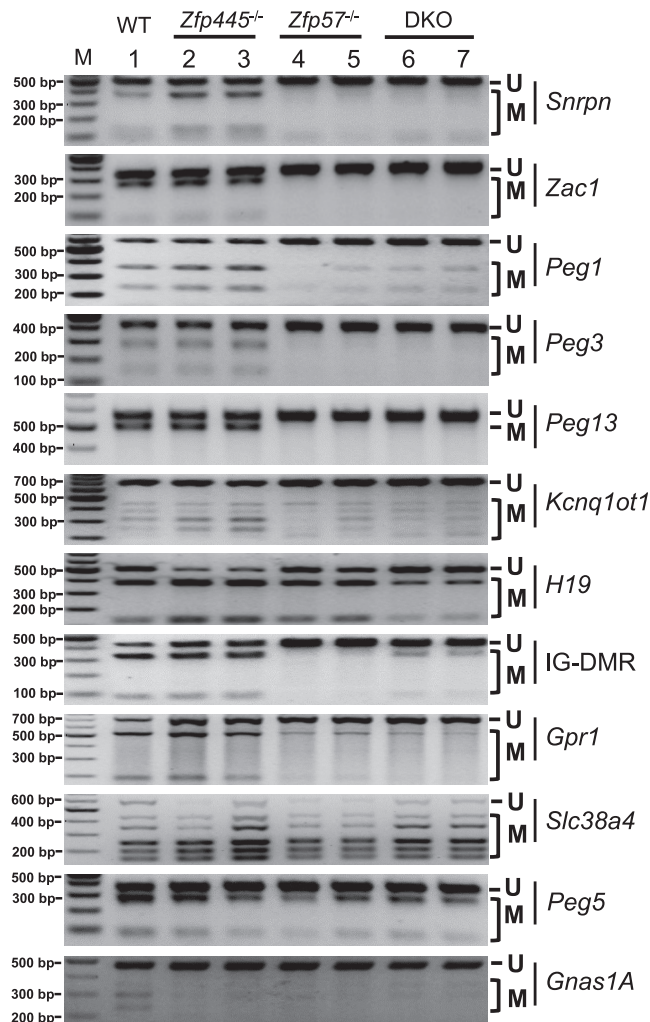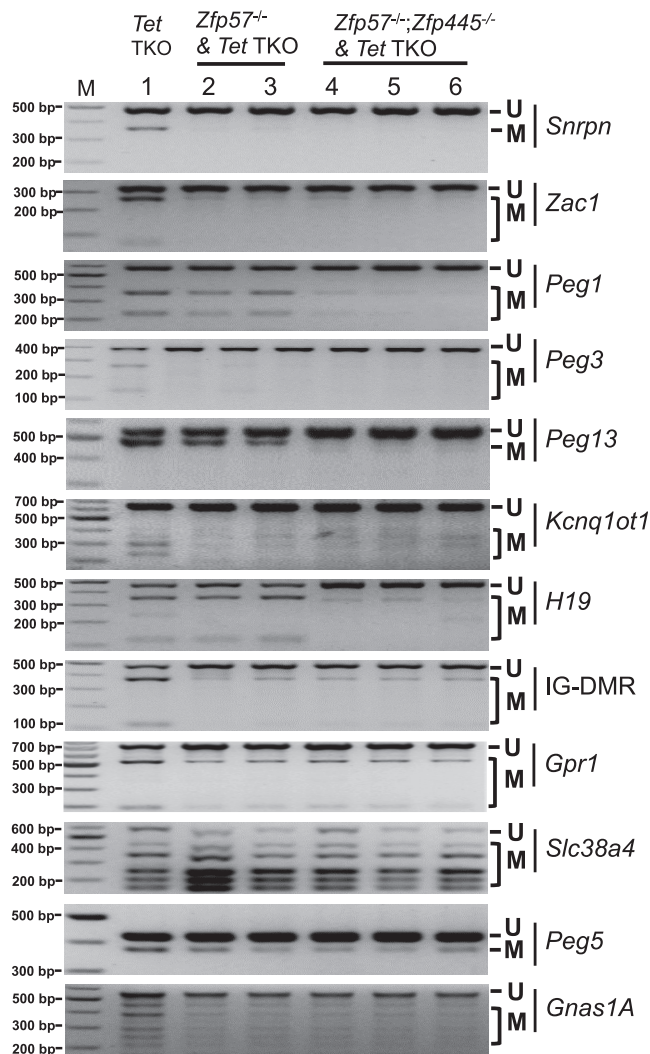
Figure 1. ZFP57 is required for the maintenance of DNA methylation imprint at most known imprinted regions in mouse embryonic stem cells based on COBRA

Genomic DNA samples were isolated from the mutant ES clones and wild-type control ES clones. Then they were subjected to COBRA analysis to examine DNA methylation at some known imprinted regions. Lane 1, wild-type (WT) ES clone. Lane 2-3, two $Zfp445^{-/-}$ mutant ES clones ($Zfp445$ KO-1 and $Zfp445$ KO-2) with deletion mutation at $Zfp445$. Lane 4-5, two $Zfp57^{-/-}$ mutant ES clones ($Zfp57$ KO-1 and $Zfp57$ KO-2) with deletion mutation at $Zfp57$. Lane 6-7, two DKO mutant ES clones (ZFP DKO-1 and ZFP DKO-2) with deletion mutations at $Zfp57$ and $Zfp445$. U, unmethylated product after COBRA. M, methylated product after COBRA. The restriction enzymes used for COBRA are as follows: $Snrpn$, $HhaI$; $Zac1$, $Taq^{\alpha}I$; $Peg1$, $Taq^{\alpha}I$; $Peg3$, $Taq^{\alpha}I$; $Peg13$, $Taq^{\alpha}I$; $Kcnq1ot1$, $Taq^{\alpha}I$; $H19$, $ClaI$; IG-DMR, $Taq^{\alpha}I$; $Gpr1$, $Taq^{\alpha}I$; $Slc38a4$, $Taq^{\alpha}I$; $Peg5$, $HhaI$; $Gnas1A$, $ClaI$.

ICR in $Zfp445^{-/-}$, $Zfp57^{-/-}$ or $Zfp57^{-/-}$; $Zfp445^{-/-}$ (DKO) mutant ES clones compared with the WT ES clone (Figure 1). Interestingly, DNA methylation was not lost at $H19$ ICR in $Zfp57^{-/-}$ mutant ES clones, but it seemed to be increased at $H19$ ICR in $Zfp445^{-/-}$ mutant ES clones compared with the WT ES clone (Figure 1). It was partially lost at $H19$ ICR in $Zfp57^{-/-}$; $Zfp445^{-/-}$ (DKO) mutant ES clones compared with the WT ES clone (Figure 1). Taken together, ZFP57 but not ZFP445 is required for the maintenance of DNA methylation at most examined ICRs in mouse ES cells.

TET proteins may not be essential for the maintenance of DNA methylation imprint in mouse embryonic stem cells

To test if loss of DNA methylation at the ICRs caused by loss of ZFP57 could be prevented in mouse ES cells when TET proteins are absent, we eliminated ZFP57 in Tet TKO ES cells ($Zfp57^{-/-}$ & Tet TKO, Lane

Figure 2. Loss of TET proteins does not prevent loss of DNA methylation imprint caused by loss of ZFP57 in mouse embryonic stem cells based on COBRA analysis

Genomic DNA samples were isolated from the *Zfp57*$^{-/-}$ mutant ES clones and the parental control *Tet* TKO ES clone. Then they were subjected to COBRA analysis to examine DNA methylation at some known imprinted regions. Lane 1, the parental *Tet* TKO ES clone lacking TET1, TET2, and TET3. Lane 2-3, two *Zfp57*$^{-/-}$ in *Tet* TKO (*Zfp57*$^{-/-}$ & *Tet* TKO) ES clones with the deletion mutation at *Zfp57* (*Zfp57* KO-3 and *Zfp57* KO-4). Lane 4-6, three *Zfp57*$^{-/-}$; *Zfp445*$^{-/-}$ in *Tet* TKO (*Zfp57*$^{-/-}$; *Zfp445*$^{-/-}$ & *Tet* TKO) ES clones with the deletion mutations at both *Zfp57* and *Zfp445* (ZFP DKO-3, ZFP DKO-4, and ZFP DKO-5). U, unmethylated product after COBRA. M, methylated product after COBRA. The restriction enzymes used for COBRA are as follows: *Snrpn*, *HhaI*; *Zac1*, *Taq*^{α}*I*; *Peg1*, *Taq*^{α}*I*; *Peg3*, *Taq*^{α}*I*; *Peg13*, *Taq*^{α}*I*; *Kcnq1ot1*, *Taq*^{α}*I*; *H19*, *ClaI*; IG-DMR, *Taq*^{α}*I*; *Gpr1*, *Taq*^{α}*I*; *Slc38a4*, *Taq*^{α}*I*; *Peg5*, *HhaI*; *Gnas1A*, *ClaI*.

2-3 of Figure 2) using CRISPR-Cas9 (Table S2) (Figure S1A) (Hu et al., 2014). There was no detectable wild-type ZFP57 in these *Zfp57* mutant ES clones on Western blot (Figure S2A). We also removed both ZFP57 and ZFP445 in *Tet* TKO ES cells (*Zfp57*$^{-/-}$; *Zfp445*$^{-/-}$ & *Tet* TKO, Lane 4-6 of Figure 2) using CRISPR-Cas9 (Table S2) (Figures S1A and S1B). *Tet* TKO ES cells lack all three TET proteins (TET1, TET2, and TET3) involved in active DNA demethylation (Hu et al., 2014). We found DNA methylation was still lost at the ICRs of *Snrpn*, *Zac1* and *Peg3* imprinted regions in *Zfp57*$^{-/-}$ or *Zfp57*$^{-/-}$; *Zfp445*$^{-/-}$ mutant *Tet* TKO ES clones even in the absence of all three TET proteins (Figure 2). DNA methylation was partially lost at the ICRs of *Peg1*, *Kcnq1ot1*, IG-DMR of *Dlk1-Dio3* imprinted region, *Gpr1*, *Peg5,* and *Gnas1A* in these mutant ES clones compared with the parental *Tet* TKO ES cells (Figure 2). At *Peg13* ICR, it was partially lost in *Zfp57*$^{-/-}$ mutant *Tet* TKO ES clones (Lane 2-3 of Figure 2) but completely lost in

$Zfp57^{-/-}$; $Zfp445^{-/-}$ mutant *Tet* TKO ES clones (Lane 4-6 of Figure 2). DNA methylation was not lost at *H19* ICR in $Zfp57^{-/-}$ mutant *Tet* TKO ES clones (Lane 2-3 of Figure 2), but largely lost in $Zfp57^{-/-}$; $Zfp445^{-/-}$ mutant *Tet* TKO ES clones (Lane 4-6 of Figure 2). There was no loss of DNA methylation at the *Slc38a4* ICR in $Zfp57^{-/-}$ or $Zfp57^{-/-}$; $Zfp445^{-/-}$ mutant *Tet* TKO ES clones, similar to $Zfp57^{-/-}$ and $Zfp57^{-/-}$; $Zfp445^{-/-}$ (DKO) mutant ES clones (Figures 1 and 2). Based on these results, it seems that loss of TET proteins could not prevent loss of DNA methylation at the ICRs caused by loss of ZFP57 or loss of both ZFP57 and ZFP445 in mouse ES cells. Therefore, we think TET proteins may not play significant roles in the stable maintenance of DNA methylation at the ICRs in mouse ES cells.

Generation of mutant embryonic stem cell clones lacking DNA methyltransferases in mouse embryonic stem cells

We have proposed that ZFP57 may recruit DNA methyltransferases through its cofactor KAP1/TRIM28 to maintain DNA methylation at the imprinted regions in ES cells in a previous study (Zuo et al., 2012). As TET proteins do not seem to be essential for the maintenance of DNA methylation imprint in mouse ES cells, we wonder if ZFP57-mediated recruitment of DNA methyltransferases may be the primary pathway in maintaining DNA methylation at the ICRs in mouse ES cells. Thus, we generated a series of *Dnmt* mutant ES clones using CRISPR-Cas9, with 2 sgRNA constructs per target gene, in the 129/DBA hybrid D1911 ES cell line (Tables S1 and S3). These include $Dnmt1^{-/-}$, $Dnmt3a^{-/-}$; $Dnmt3b^{-/-}$ (DKO), and $Dnmt1^{-/-}$; $Dnmt3a^{-/-}$; $Dnmt3b^{-/-}$ (TKO) mutant ES clones. As UHRF1 has been shown to be a major partner for DNMT1 in maintaining DNA methylation, we also created $Uhrf1^{-/-}$ mutant (*Uhrf1* KO) ES clones to test if it functions in the same pathway as DNMT1 in maintaining DNA methylation in ES cells (Tables S1 and S4) (Figure S1F). There was no detectable DNMT1, UHRF1, DNMT3A, or DNMT3B in the corresponding mutant ES clones on Western blots (Figure S2). As controls, two WT ES clones (WT-1 and WT-2) were also individually picked from the ES cell culture transfected with the empty pX330 vector. High levels of OCT4 and NANOG were detected in the ES culture of these mutant ES clones and the WT ES clones by immunostaining (Figures S3 and S4).

DNMT1 and UHRF1 were required for maintaining DNA methylation at the examined imprinting control regions in mouse embryonic stem cells based on COBRA

Genomic DNA samples were isolated from *Dnmt* mutant, *Uhrf1* mutant, and WT ES clones at Passage 4 (P4) (see STAR Methods). Then they were subjected to COBRA analysis to examine DNA methylation at some known ICRs (Figure 3). We found DNA methylation was completely lost at the ICRs of the *Snrpn*, *Zac1*, *Peg1*, *Peg3*, *Peg13*, *Kcnq1ot1*, and *H19* in two *Dnmt1* KO mutant ES clones at P4 compared with two WT ES clones at P4 (Figure 3). DNA methylation was partially lost at the IG-DMR of the *Dlk1-Dio3* imprinted region as well as the ICRs of *Gpr1*, *Slc38a4*, *Peg5*, and *Gnas1A* in the *Dnmt1* KO mutant ES clones at P4 (Figure 3). Almost identical COBRA results were observed at these ICRs in two *Uhrf1* KO ES clones at P4. Complete loss of DNA methylation was observed at the ICRs of the *Snrpn*, *Zac1*, *Peg1*, *Peg3*, *Peg13*, *Kcnq1ot1*, and *H19*, whereas there was partial loss of DNA methylation at the IG-DMR of *Dlk1-Dio3* imprinted region, *Gpr1*, *Slc38a4*, *Peg5*, and *Gnas1A* ICRs in the *Uhrf1* KO ES clones at P4 (Figure 3). These results indicate that both DNMT1 and UHRF1 are necessary for the maintenance of DNA methylation at these examined ICRs in mouse ES cells and they are likely to function in the same complex or pathway in maintaining ICR DNA methylation in mouse ES cells as expected.

DNA methylation was partially lost at a few imprinting control regions in *Dnmt3* mutant embryonic stem cells based on COBRA

There was no loss of DNA methylation at the ICRs of the *Snrpn*, *Zac1*, *Peg1*, *Peg3*, *Peg13*, *Kcnq1ot1*, and *H19* in two *Dnmt3* DKO mutant ES clones at P4 compared with two WT ES clones at P4 (Figure 3). Interestingly, DNA methylation was partially lost at the ICRs of the IG-DMR of the *Dlk1-Dio3* imprinted region, *Gpr1*, *Slc38a4*, *Peg5*, and *Gnas1A* in *Dnmt3* DKO mutant ES clones at P4 (Figure 3). Actually, loss of DNA methylation appeared to be more severe at *Peg5* and *Gnas1A* ICRs in two *Dnmt3* DKO mutant ES clones than in the *Dnmt1* KO or *Uhrf1* KO mutant ES clones, in comparison to two WT control ES clones. These results suggest that DNMT3A and DNMT3B may be partially redundant with DNMT1 in maintaining DNA methylation at a subset of known ICRs in mouse ES cells. This hypothesis is confirmed by the DNA methylation results obtained with whole genome bisulfite sequencing (WGBS) analysis of these ES clones with over 99% of bisulfite conversion rate of each sample (Table S5). These data have allowed us to perform
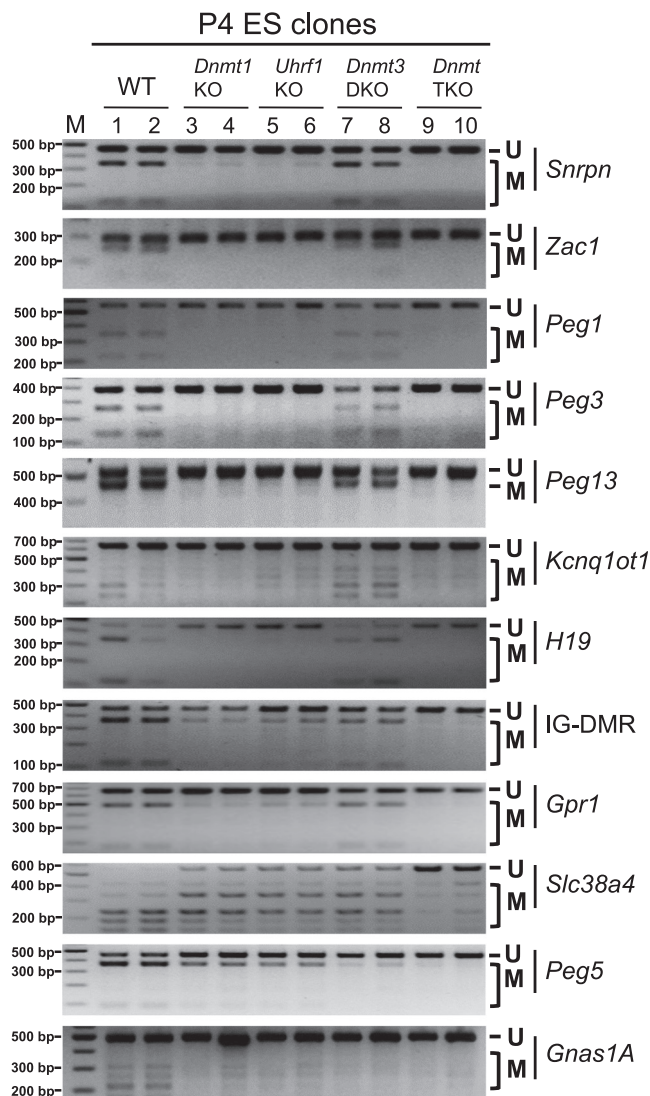
Figure 3. DNMT1, as well as DNMT3A and DNMT3B, are involved in the maintenance of DNA methylation imprint in mouse embryonic stem cells based on COBRA analysis

Genomic DNA samples were isolated from the *Dnmt* mutant ES clones at early passage (P4) and the wild-type (WT) control ES clones at P4. Then they were subjected to COBRA analysis to examine DNA methylation at some known imprinted regions. Lane 1-2, two WT ES clones (WT-1 and WT-2) that were isolated from singly picked ES clones after transfection with empty pX330. Lane 3-4, two *Dnmt1*$^{-/-}$ mutant ES clones (*Dnmt1* KO-1 and *Dnmt1* KO-2) with deletion mutation at *Dnmt1*. Lane 5-6, two *Uhrf1*$^{-/-}$ mutant ES clones (*Uhrf1* KO-1 and *Uhrf1* KO-2) with deletion mutation at *Uhrf1*. Lane 7-8, two *Dnmt3* DKO mutant ES clones (*Dnmt3* DKO-1 and *Dnmt3* DKO-2) with deletion mutations at both *Dnmt3a* and *Dnmt3b*. Lane 9-10, two *Dnmt* TKO mutant ES clones (*Dnmt* TKO-1 and *Dnmt* TKO-2) with deletion mutations at *Dnmt1*, *Dnmt3a*, and *Dnmt3b*. U, unmethylated product after COBRA. M, methylated product after COBRA. The restriction enzymes used for COBRA are as follows: *Snrpn*, *Hha*I; *Zac1*, *Taq*$^{\alpha}$I; *Peg1*, *Taq*$^{\alpha}$I; *Peg3*, *Taq*$^{\alpha}$I; *Peg13*, *Taq*$^{\alpha}$I; *Kcnq1ot1*, *Taq*$^{\alpha}$I; *H19*, *Cla*I; IG-DMR, *Taq*$^{\alpha}$I; *Gpr1*, *Taq*$^{\alpha}$I; *Slc38a4*, *Taq*$^{\alpha}$I; *Peg5*, *Hha*I; *Gnas1A*, *Cla*I.

more in-depth analyses of DNA methylation at the ICRs as well as the DMRs, repeats, and other genomic regions as illustrated later in discussion (Tables S6–S9).

DNMT1 played major role in maintaining DNA methylation at most known imprinting control regions in mouse embryonic stem cells according to whole genome bisulfite sequencing

To confirm the COBRA results for *Dnmt* and *Uhrf1* mutant ES clones, we analyzed WGBS data of two independent ES clones of *Dnmt* and *Uhrf1* mutant ES cells as well as two WT ES clones at P4 to examine DNA
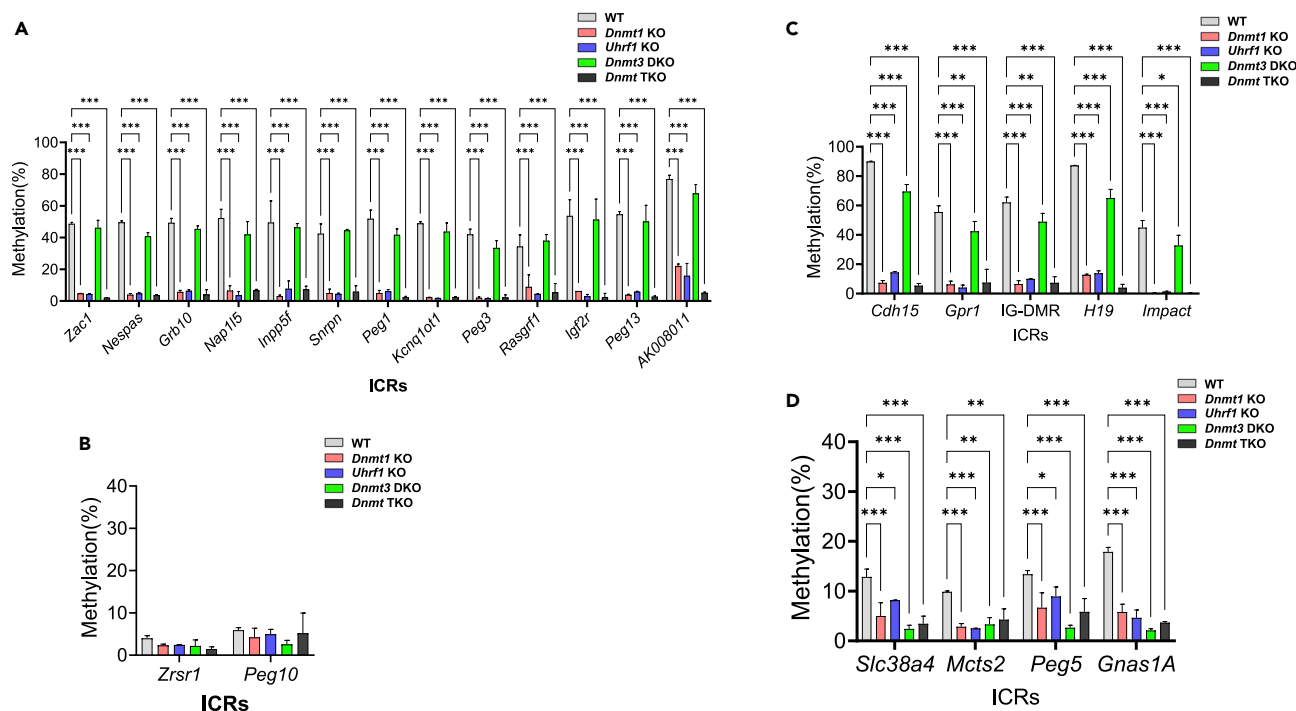
Figure 4. DNA methyltransferases are differentially required for the maintenance of DNA methylation imprint at the known imprinted regions in mouse ES cells according to WGBS analysis

Genomic DNA samples were isolated from the *Dnmt* and *Uhrf1* mutant ES clones as well as the wild-type (WT) control ES clones at early passage (P4). Then they were subjected to whole genome bisulfite sequencing (WGBS) analysis to examine DNA methylation at the known imprinted regions and other genomic regions. The percentages (%) of DNA methylation were calculated for the ICRs of the known imprinted regions. WT, wild-type ES clone (gray). *Dnmt1* KO, *Dnmt1* mutant ES clone (orange red). *Uhrf1* KO, *Uhrf1* mutant ES clone (blue). *Dnmt3* DKO, *Dnmt3a$^{-/-}$*; *Dnmt3b$^{-/-}$* DKO mutant ES clone (green). *Dnmt* TKO, *Dnmt* TKO mutant ES clone (black) with deletion mutations at *Dnmt1*, *Dnmt3a*, and *Dnmt3b*. Two-way ANOVA was carried out in statistical analysis, with Dunnett multiple comparison test, for DNA methylation at the ICRs comparing two ES clones of each *Dnmt* or *Uhrf1* mutant ES cells with two WT ES clones. The data were presented as mean $\pm$ SEM with the following statistical significance values: *$p < 0.05$; **$p < 0.01$; ***$p < 0.001$.
(A) DNMT1 maintained DNA methylation imprint at most imprinting control regions (ICRs) in mouse ES cells. These include *Zac1*, *Nespas*, *Grb10*, *Nap1l5*, *Inpp5f*, *Snrpn*, *Peg1*, *Kcnq1ot1*, *Peg3*, *Rasgrf1*, *Igf2r*, *Peg13*, and *AK008011*.
(B) There was little DNA methylation at the *Zrsr1* and *Peg10* ICRs in the *Dnmt* mutant and wild-type control mouse ES cells.
(C) DNMT1 played major roles in maintaining DNA methylation imprint at five ICRs in mouse ES cells, whereas there was a significant loss of DNA methylation at these five ICRs in the *Dnmt3* DKO mutant ES cells. These ICRs include *Cdh15*, *Gpr1*, IG-DMR of the *Dlk1-Dio3* imprinted region, *H19* and *Impact*.
(D) DNMT3A and DNMT3B played equally or more important roles than DNMT1 in the maintenance of DNA methylation imprint at the *Slc38a4*, *Mcts2*, *Peg5*, and *Gnas1A* ICRs in mouse ES cells.

methylation at all known imprinted regions (Tables S6 and S7) (Figure 4). Indeed, we found DNA methylation was almost completely lost at the ICRs of the *Zac1*, *Nespas*, *Grb10*, *Nap1l5*, *Inpp5f*, *Snrpn*, *Peg1*, *Kcnq1ot1*, *Peg3*, *Rasgrf1*, *Igf2r* and *Peg13* in the *Dnmt1* KO or *Uhrf1* KO ES clones, similar to *Dnmt* TKO ES clones (Figure 4A) (Table 1). There was some DNA methylation remaining at the *AK008011* ICR in the *Dnmt1* KO or *Uhrf1* KO ES clones, compared with *Dnmt* TKO ES clones (Figure 4A) (Table 1). By contrast, there was no significant loss of DNA methylation at these ICRs in the *Dnmt3* DKO mutant ES clones compared with two WT ES clones (Figure 4A) (Table 1). There was little DNA methylation at the *Zrsr1* and *Peg10* ICRs in mouse ES cells, and therefore it is difficult to assess how DNA methylation may be maintained at these two ICRs in the *Dnmt* and *Uhrf1* mutant ES clones (Figure 4B) (Table 1). DNA methylation was also largely lost at the ICRs of *Cdh15*, *Gpr1*, IG-DMR of the *Dlk1-Dio3* imprinted region, *H19* and *Impact* in the *Dnmt1* KO or *Uhrf1* KO or *Dnmt* TKO ES clones, although there was significant loss of DNA methylation at these ICRs in the *Dnmt3* DKO mutant ES clones compared with two WT ES clones (Figure 4C) (Table 1). Taken together, these results indicate that DNMT1 is the major DNA methyltransferase in maintaining ICR DNA methylation at most known imprinted regions in mouse ES cells. This finding is confirmed by the Integrative Genomics Viewer (IGV) plots of DNA methylation at these ICRs in these ES clones (Figure 5).

Table 1. The effects of DNMTs or UHRF1 on ICR DNA methylation in ES cells

ICR	*Dnmt1* KO ES (DNMT1 function)	*Uhrf1* KO ES (UHRF1 function)	*Dnmt3* DKO ES (DNMT3A/3B function)	*Dnmt* TKO
Zac1	Lost (Yes)	Lost (Yes)	No loss (No)	Lost
Nespas	Lost (Yes)	Lost (Yes)	No loss (No)	Lost
Grb10	Lost (Yes)	Lost (Yes)	No loss (No)	Lost
Nap1l5	Lost (Yes)	Lost (Yes)	No loss (No)	Lost
Inpp5f	Lost (Yes)	Lost (Yes)	No loss (No)	Lost
Snrpn	Lost (Yes)	Lost (Yes)	No loss (No)	Lost
Peg1	Lost (Yes)	Lost (Yes)	No loss (No)	Lost
Kcnq1ot1	Lost (Yes)	Lost (Yes)	No loss (No)	Lost
Peg3	Lost (Yes)	Lost (Yes)	No loss (No)	Lost
Rasgrf1	Lost (Yes)	Lost (Yes)	No loss (No)	Lost
Igf2r	Lost (Yes)	Lost (Yes)	No loss (No)	Lost
Peg13	Lost (Yes)	Lost (Yes)	No loss (No)	Lost
AK008011	Mostly lost (Yes)	Mostly lost (Yes)	No loss (Minor[c])	Lost
Cdh15	Lost (Yes)	Mostly lost (Yes)	Partial loss (Yes)	Lost
Gpr1	Lost (Yes)	Lost (Yes)	Partial loss (Yes)	Lost
IG-DMR	Lost (Yes)	Lost (Yes)	Partial loss (Yes)	Lost
H19	Mostly lost (Yes)	Mostly lost (Yes)	Partial loss (Yes)	Lost
Impact	Lost (Yes)	Lost (Yes)	Partial loss (Yes)	Lost
[a]*Zrsr1*	Low (NA)	Low (NA)	Low (NA)	Low (NA)
[a]*Peg10*	Low (NA)	Low (NA)	Low (NA)	Low (NA)
[b]*Slc38a4*	Partial loss (Yes)	Partial loss (Yes)	Lost (Yes)	Lost
[b]*Mcts2*	Lost (Yes)	Lost (Yes)	Lost (Yes)	Lost
[b]*Peg5*	Partial loss (Yes)	Partial loss (Yes)	Lost (Yes)	Lost
[b]*Gnas1A*	Mostly lost (Yes)	Mostly lost (Yes)	Lost (Yes)	Lost

Note: NA, not applicable.
[a]methylation was very low (around 5%) at this ICR in WT ES cells.
[b]methylation was relatively low (<20%) at this ICR in WT ES cells.
[c]DNMT3A and DNMT3B appeared to have minor roles at the *AK008011* ICR as DNA methylation was partially lost in the *Dnmt1* KO or *Uhrf1* KO ES clones but complete missing in the *Dnmt* TKO ES clones (Figure 4A).

DNMT3A and DNMT3B contributed to the maintenance of DNA methylation at a subset of imprinting control regions in mouse embryonic stem cells according to whole-genome bisulfite sequencing

Despite that DNMT1 played major roles in maintaining DNA methylation at most known ICRs in mouse ES cells, loss of DNMT3A and DNMT3B caused significant loss of DNA methylation at *Cdh15*, *Gpr1*, IG-DMR of the *Dlk1-Dio3* imprinted region, *H19* and *Impact* ICRs in mouse ES cells (Figure 4C) (Table 1). Furthermore, they were also required for the maintenance of DNA methylation at the *Slc38a4*, *Mcts2*, *Peg5,* and *Gnas1A* ICRs in mouse ES cells (Figure 4D) (Table 1). Interestingly, DNMT3A and DNMT3B appeared to play no less important roles than DNMT1 in maintaining DNA methylation at these ICRs because DNA methylation was similarly or more severely lost at *Slc38a4*, *Mcts2*, *Peg5,* and *Gnas1A* ICRs in the *Dnmt3* DKO mutant ES clones than in the *Dnmt1* KO or *Uhrf1* KO ES clones, in comparison to two *Dnmt* TKO and two WT ES clones (Figure 4D) (Table 1). These results are easily visible by the DNA methylation IGV plots at these ICRs in these ES clones (Figure 5). A similar loss of DNA methylation at the *Slc38a4*, *Peg5* and *Gnas1A* ICRs was found in the COBRA analysis of *Dnmt* and *Uhrf1* mutant ES clones compared with two WT ES clones (Figure 3). Therefore, DNMT3A and DNMT3B are essential for maintaining DNA methylation at a subset of ICRs in mouse ES cells.

Maintenance of germline-derived imprinting control region methylation by DNMT1 as well as DNMT3A and DNMT3B in mouse embryonic stem cells

It appeared that DNMT3A and DNMT3B, together with DNMT1, were involved in maintaining DNA methylation at the ICRs in mouse ES cells. We wondered if germline-derived ICR methylation was, indeed,
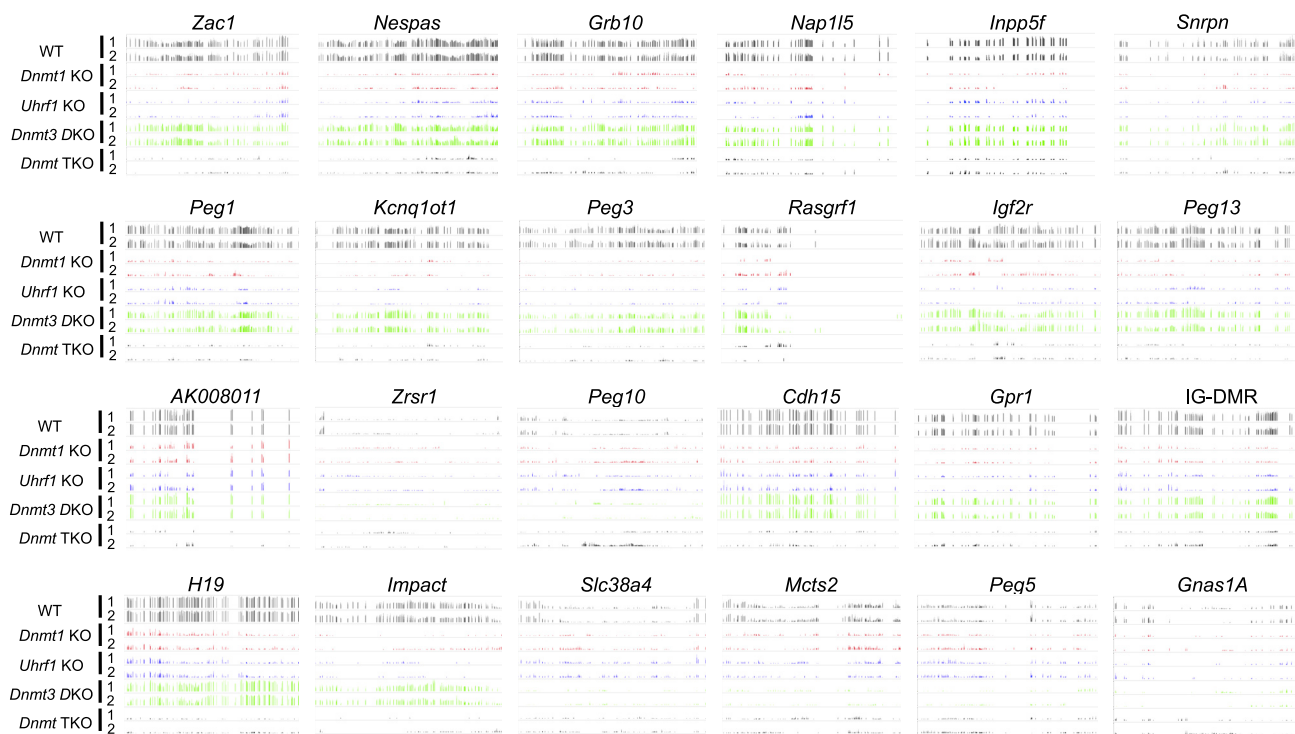
Figure 5. Loss of DNA methylation imprint was confirmed at the known ICRs in *Dnmt* mutant ES clones based on the methylation IGV plot
Genomic DNA samples isolated from two independent ES clones (1 and 2) of *Dnmt* mutant, *Uhrf1* mutant, and wild-type (WT) control ES cells at P4 were subjected to whole genome bisulfite sequencing (WGBS) analysis. IGV methylation plots were obtained to examine DNA methylation at 24 known ICRs that include *Zac1*, *Nespas*, *Grb10*, *Nap1l5*, *Inpp5f*, *Snrpn*, *Peg1*, *Kcnq1ot1*, *Peg3*, *Rasgrf1*, *Igf2r*, *Peg13*, *AK008011*, *Zrsr1*, *Peg10*, *Cdh15*, *Gpr1*, IG-DMR of the *Dlk1-Dio3* imprinted region, *H19*, *Impact*, *Slc38a4*, *Mcts2*, *Peg5*, and *Gnas1A*. WT, wild-type ES clone (gray). *Dnmt1* KO, *Dnmt1* mutant ES clone (orange red). *Uhrf1* KO, *Uhrf1* mutant ES clone (blue). *Dnmt3* DKO, *Dnmt3a*$^{-/-}$; *Dnmt3b*$^{-/-}$ DKO mutant ES clone (green). *Dnmt* TKO, *Dnmt* TKO mutant ES clone (black) with deletion mutations at *Dnmt1*, *Dnmt3a*, and *Dnmt3b*. All methylation IGV plots have the same scale (0-100) in this figure.

maintained by three DNA methyltransferases in mouse ES cells. For this, we took advantage of the SNPs present in the parental D1911 ES clone that was derived from the timed mating between a 129S6/SvEvTac (129) female mouse and a DBA2/J (DBA) male mouse (Lau et al., 2016b). Allelic DNA methylation analysis was performed to examine how germline-derived DNA methylation imprint is maintained at the ICRs with a maternal 129 allele and a paternal DBA allele in mouse ES cells (Table S9) (Figure 6).

DNA methylation imprint at the ICRs of *H19*, *Rasgrf1*, and IG-DMR of the *Dlk1-Dio3* imprinted region is established during spermatogenesis and stably maintained on the paternal chromosomes in somatic cells after fertilization. For other known ICRs, DNA methylation imprint is reset during oogenesis and stably maintained on the maternal chromosomes. In the WT ES cells of this study, DNA methylation imprint is located at the ICRs of *H19*, *Rasgrf1*, and IG-DMR of the *Dlk1-Dio3* imprinted region on the paternal DBA chromosomes, whereas it is at other known ICRs on the maternal 129 chromosomes (Figure 6).

We found germline-derived ICR methylation was almost completely lost at the ICRs of *Zac1*, *Peg13*, *Nespas*, *Snrpn*, and *Inpp5f* on the maternal 129 chromosomes in the *Dnmt1* KO or *Uhrf1* KO ES clones, similar to *Dnmt* TKO ES clones (Figure 6A) (Table 2). In contrast, there was no significant loss of DNA methylation at these ICRs in the *Dnmt3* DKO mutant ES clones in comparison to two WT control ES clones (Figure 6A) (Table 2). DNA methylation was lost at the *Impact* and *Cdh15* ICRs on the maternal 129 chromosomes in the *Dnmt1* KO or *Uhrf1* KO ES clones. Nevertheless, there was also a significant loss of DNA methylation at these two ICRs in the *Dnmt3* DKO mutant ES clones compared with two WT ES clones (Figure 6B) (Table 2). Surprisingly, high level of DNA methylation was observed at the *Cdh15* ICR on the paternal DBA chromosome in two WT ES clones that were largely lost in the *Dnmt1* KO or *Uhrf1* KO ES clones but also significantly reduced in the *Dnmt3* DKO mutant ES clones compared with two WT ES clones (Figure 6B) (Table 2). As expected, germline-derived ICR methylation was completely lost at these ICRs on the maternal 129
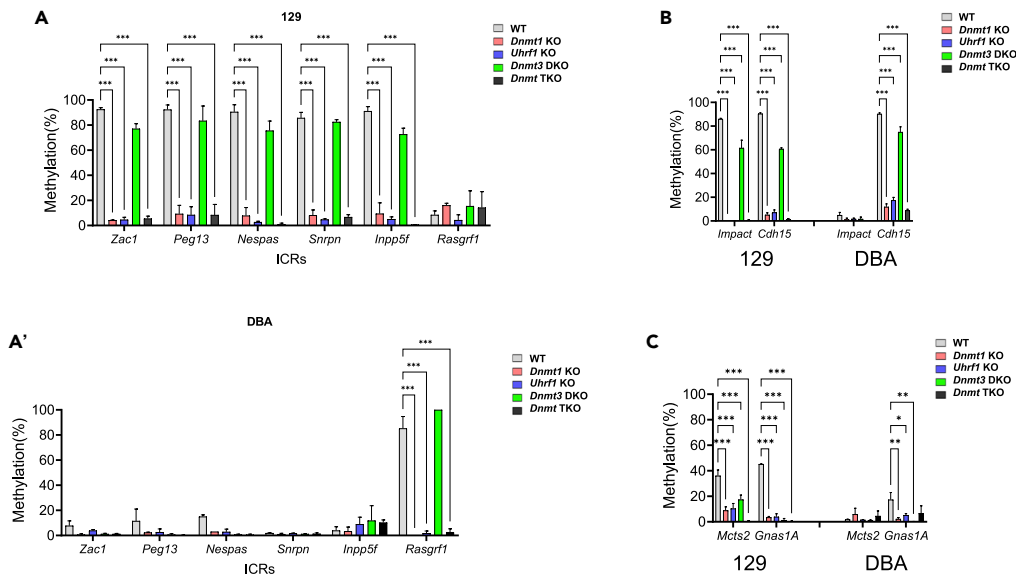
Figure 6. DNMT3A and DNMT3B, together with DNMT1, maintain germline-derived DNA methylation imprint in a subset of known ICRs in mouse embryonic stem cells according to allelic DNA methylation analysis

Genomic DNA samples isolated from the mutant ES clones and the wild-type control ES clones were subjected to whole genome bisulfite sequencing (WGBS) analysis to examine DNA methylation at the known ICRs. The percentages (%) of DNA methylation were determined for the paternal (DBA) or maternal (129) ICR in mouse ES clones based on the SNPs present at a subset of ICRs. WT, wild-type ES clone (gray). *Dnmt1* KO, *Dnmt1* mutant ES clone (orange red). *Uhrf1* KO, *Uhrf1* mutant ES clone (blue). *Dnmt3* DKO, *Dnmt3a*−/−; *Dnmt3b*−/− DKO mutant ES clone (green). *Dnmt* TKO, *Dnmt* TKO mutant ES clone (black) with deletion mutations at *Dnmt1*, *Dnmt3a*, and *Dnmt3b*. For statistical analysis of the allelic DNA methylation data obtained for the 129 or DBA alleles of the ICRs with SNPs, two-way ANOVA with Dunnett multiple comparison test was applied to two ES clones of each *Dnmt* or *Uhrf1* mutant ES cells in comparison with two WT ES clones. The values in the graphs were presented as mean ± SEM with the following statistical significance: *p < 0.05; **p < 0.01; ***p < 0.001. A) The percentages (%) of DNA methylation were determined for the maternal (129) ICR based on the SNPs present at *Zac1*, *Peg13*, *Nespas*, *Snrpn*, *Inpp5f*, and *Rasgrf1* ICRs.

(A') The percentages (%) of DNA methylation was determined for the paternal (DBA) ICR based on the SNPs present at *Zac1*, *Peg13*, *Nespas*, *Snrpn*, *Inpp5f*, and *Rasgrf1* ICRs.

(B) The percentages (%) of DNA methylation were determined for the maternal (129) or paternal (DBA) ICR at the *Impact* and *Cdh15* ICRs in which DNMT3A and DNMT3B contributed a minor role to the maintenance of DNA methylation in mouse ES cells.

(C) The percentages (%) of DNA methylation were determined for the maternal (129) or paternal (DBA) ICR at the *Mcts2* and *Gnas1A* ICRs in mouse ES cells. DNMT3A and DNMT3B played equally important roles as DNMT1 in the maintenance of germline-derived DNA methylation imprint at the maternal 129 ICRs of the *Mcts2* and *Gnas1A* imprinted regions.

chromosomes in the *Dnmt* TKO ES cells (Figures 6A and 6B) (Table 2). Taken together, DNMT1 played major roles in maintaining germline-derived methylation at these ICRs on the maternal chromosomes in mouse ES cells. Interestingly, DNMT3A and DNMT3B contributed to the maintenance of germline-derived methylation at the *Impact* and *Cdh15* ICRs on the maternal 129 chromosomes, which is consistent with their functions in maintaining overall DNA methylation at these two ICRs (Figures 4C and 6B).

DNA methylation imprint was present at the *Rasgrf1* ICR on the paternal DBA chromosome in the WT or *Dnmt3* DKO ES cells (Figure 6A') (Table 2). There was no detectable DNA methylation at the *Rasgrf1* ICR on the paternal DBA chromosome in the *Dnmt1* KO or *Uhrf1* KO or *Dnmt* TKO ES cells (Figure 6A'). Low level of DNA methylation was similarly observed at the *Rasgrf1* ICR on the maternal 129 chromosome in the WT, *Dnmt1* KO, *Dnmt3* DKO, and *Dnmt* TKO ES cells (Figure 6A'). It seemed that DNMT1 but not DNMT3A and DNMT3B were required for maintaining DNA methylation imprint at the *Rasgrf1* ICR on the paternal chromosome in mouse ES cells.

Intriguingly, DNA methylation was largely lost at the *Mcts2* ICR and completely lost at the *Gnas1A* ICR on the maternal 129 chromosomes in the *Dnmt1* KO or *Uhrf1* KO or *Dnmt3* DKO ES cells, compared with the WT ES cells (Figure 6C) (Table 2). There was low level of DNA methylation at the *Gnas1A* ICR on the paternal DBA

Table 2. Allelic DNA methylation at the ICRs in the WT and mutant ES cells

ICR	WT ES	*Dnmt1* KO	*Uhrf1* KO	*Dnmt3* DKO	*Dnmt* TKO
Zac1 (M)	Me (M)	Me lost	Me lost	No Loss (M)	Me lost
Peg13 (M)	Me (M)	Me lost	Me lost	No Loss (M)	Me lost
Nespas (M)	Me (M)	Me lost	Me lost	No Loss (M)	Me lost
Snrpn (M)	Me (M)	Me lost	Me lost	No Loss (M)	Me lost
Inpp5f (M)	Me (M)	Me lost	Me lost	No Loss (M)	Me lost
Rasgrf1 (P)	Me (P)	Low Me? (M) Me lost (P)	Me lost (P)	Low Me? (M) No Loss (P)	Low Me? (M) Me lost (P)
Impact (M)	Me (M)	Me lost	Me lost	Partial Loss (M)	Me lost
Cdh15 (M)[a]	Me (M) Me (P)	Me lost (M) Me lost (P)	Me lost (M) Low Me? (P)	Partial Loss (M) Partial Loss (P)	Me lost (M) Me lost (P)
Mcts2 (M)	Me (M)	Partial Loss (M)	Partial Loss (M)	Partial Loss (M)	Me lost
Gnas1A (M)[b]	Me (M) Low Me (P)	Me lost (M) Me lost (P)	Me lost (M) Me lost (P)	Me lost (M) Me lost (P)	Me lost (M) Me lost (P)

M, maternal allele. P, paternal allele. Me, methylation. All ICRs in this table were reported to contain germline-derived DNA methylation on the maternal chromosomes except that *Rasgrf1* ICR is reported to be methylated on the paternal chromosome.

[a]both maternal and paternal ICRs were similarly methylated in the WT ES cells.

[b]maternal and paternal ICRs had different levels of methylation in the WT ES cells.

chromosome in the WT ES cells that were lost in the *Dnmt1* KO or *Uhrf1* KO or *Dnmt3* DKO ES clones (Figure 6C) (Table 2). It appeared that DNMT3A and DNMT3B, together with DNMT1, maintained germline-derived DNA methylation at the *Mcts2* and *Gnas1A* ICRs on the maternal 129 chromosomes in mouse ES cells. These are also consistent with their maintenance functions in overall DNA methylation at these two ICRs (Figures 4D and 6C).

Similar observations were obtained from the allelic methylation IGV plots of these ICRs (Figure S5). Therefore, we conclude that DNMT3A and DNMT3B are required for the maintenance of germline-derived ICR methylation at a subset of ICRs in mouse ES cells although DNMT1 is the major DNA methyltransferase for maintaining germline-derived DNA methylation imprint at most ICRs in mouse ES cells.

DNA methylation at repeats and other genomic regions in mouse embryonic stem cells

Besides the ICRs and DMRs, there are many other genomic regions that can be methylated in ES cells. Therefore, we examined DNA methylation at repeats and genic regions in the mutant ES cells in comparison to the WT ES cells (Table S8) (Figure S6). Overall, roughly 70% of the CpG sites of the entire genome were methylated in two WT ES clones (Figure S6A). A bit over 20% of CpG sites remained methylated in the *Dnmt1* KO or *Uhrf1* KO ES clones, whereas close to 40% of CpG sites were methylated in the *Dnmt3* DKO mutant ES clones (Figure S6A). As expected, almost all CpG sites lost methylation in the *Dnmt* TKO ES clones (Figure S6A). These results suggest that all three DNA methyltransferases are required for maintaining CpG methylation in mouse ES cells, with DNMT1 being slightly more important than DNMT3A and DNMT3B.

Similar levels of DNA methylation (about 70-75%) were observed in the gene body, intron and intergenic regions in the WT ES cells (Figure S6B). 20-30% of CpG sites remained methylated in the gene body, intron and intergenic regions in the *Dnmt1* KO or *Uhrf1* KO ES cells while 30-40% of CpG sites were methylated in these regions in the *Dnmt3* DKO mutant ES clones (Figure S6B). It appeared that three DNA methyltransferases were necessary for maintaining DNA methylation in the gene body, intron and intergenic regions in mouse ES cells and DNMT1 played a bit more important roles than DNMT3A and DNMT3B in these regions. About 60% of the CpG sites located in the exons of the genic regions and 20-30% of the CpG sites at the promoters of the genic regions were methylated in the WT ES cells (Figure S6B). Interestingly, partial loss of DNA methylation was similarly observed at the exonic and promoter regions in *Dnmt1* KO or *Uhrf1* KO or *Dnmt3* DKO ES cells (Figure S6B). Therefore, DNMT3A and DNMT3B seemed to be as important as DNMT1 in maintaining DNA methylation in these regions in mouse ES cells.

Approximately 80% of the CpG sites located in the DNA, LINE, LTR, and SINE repeats were found to be methylated in the WT ES cells (Figure S6C). Slightly less DNA methylation was observed at the CpG sites

located in the simple repeat regions (roughly 60%) in the WT ES cells (Figure S6C). DNA methylation was almost completely absent at all repeat regions in *Dnmt* TKO ES cells. Close to 30% of CpG sites at the SINE repeats were methylated in *Dnmt1* KO or *Uhrf1* KO or *Dnmt3* DKO ES cells (Figure S6C). DNA methylation was similarly lost at the DNA, LINE, LTR, and simple repeat regions in the *Dnmt1* KO or *Uhrf1* KO ES cells, with 20-30% of the CpG sites methylated in the absence of DNMT1 or UHRF1 (Figure S6C). However, more than 40% of the CpG sites were still methylated at the DNA, LINE, LTR, and simple repeat regions in *Dnmt3* DKO ES cells (Figure S6C). These results indicate that DNMT3A and DNMT3B are only slightly less crucial than DNMT1 and UHRF1 in maintaining DNA methylation at these repeat regions.

Fewer than 10% of the CpG sites were methylated in all CpG islands (CGIs) in the WT ES clones (Figure S6D). About 5% of the CpG sites in CGIs were still methylated in the *Dnmt1* KO or *Uhrf1* KO ES clones. But there were even fewer CpG sites (less than 5%) that remained methylated in the *Dnmt3* DKO or *Dnmt* TKO ES clones. It seemed that DNMT3A and DNMT3B, together with DNMT1, are required for maintaining DNA methylation at the CGIs in mouse ES cells.

DNA methylation at somatic differentially methylated regions in mouse embryonic stem cells

We also examined DNA methylation at somatic DMRs in mouse ES cells (Figure S7) (Table S7). As expected, DNA methylation was almost completely absent at these somatic DMRs in *Dnmt* TKO ES cells (Figure S7). There were about 80% and 90% methylation at the *Smoc2* DMR and *Igf2*-DMR0, respectively, in the WT ES cells (Figure S7A). Only 20-30% of CpG sites were methylated at *Smoc2* DMR and approximately 40% of CpG sites were methylated at *Igf2*-DMR0 in the *Dnmt1* KO or *Uhrf1* KO ES clones (Figure S7A). Although there was no significant loss of DNA methylation at these two DMRs in the *Dnmt3* DKO mutant ES clones compared with two WT control ES clones, DNMT3A and DNMT3B contributed to the maintenance of DNA methylation at both *Smoc2* DMR and *Igf2*-DMR0 because little DNA methylation was observed at these two DMRs in the *Dnmt* TKO ES clones while there were 20-40% methylation at both DMRs in the *Dnmt1* KO or *Uhrf1* KO ES clones (Figure S7A).

Except for the *Meg3* DMR with around 50% methylation in the WT ES cells and little methylation in the *Dnmt1* KO or *Uhrf1* KO or *Dnmt* TKO ES clones, 70-80% of the CpG sites were methylated at the *Meg3*-Intron, *Pde10a*, *Park2* and *Slc22a2* DMRs in the WT ES cells and partial loss of DNA methylation occurred in these DMRs in the *Dnmt1* KO or *Uhrf1* KO ES clones in comparison to the WT and *Dnmt* TKO ES clones (Figure S7B). DNA methylation was also significantly lost at these five somatic DMRs in the *Dnmt3* DKO mutant ES cells (Figure S7B). Therefore, DNMT3A and DNMT3B were required for maintaining DNA methylation at these five DMRs although DNMT1 was the major maintenance DNMT for them.

About 50-80% of the CpG sites were methylated at the *Zdbf2*, *AC185554.1*, and *Gab1* DMRs in the WT ES cells (Figure S7C). Interestingly, loss of DNA methylation appeared to be more severe at these three DMRs in the *Dnmt3* DKO mutant ES clones compared with the *Dnmt1* KO or *Uhrf1* KO ES clones (Figure S7C). DNMT3A and DNMT3B played more important roles than DNMT1 in maintaining DNA methylation at these three DMRs in ES cells.

Only 10-30% of the CpG sites were methylated at the *Rian*, *Nesp*, *Igf2r*-TSS, and *Jade1* DMRs in the WT ES cells (Figure S7D). Partial loss of DNA methylation was observed at these DMRs in the *Dnmt1* KO ES clones in comparison to the WT ES clones, whereas DNA methylation was similarly lost in the *Dnmt3* DKO and *Dnmt* TKO ES clones (Figure S7D). Surprisingly, there was no loss of DNA methylation at the *Igf2r*-TSS DMR in the *Uhrf1* KO ES clones although the partial loss of DNA methylation was observed at the *Nesp* and *Jade1* DMRs in the *Uhrf1* KO ES clones. Twice of CpG sites were methylated at the *Rian* DMR in the *Uhrf1* KO ES clones compared with the *Dnmt1* KO ES clones (Figure S7D). These results indicated that three DNMTs were necessary for maintaining DNA methylation at these DMRs with low levels of methylation. DNMT1 might not always require UHRF1 for its maintenance methylation.

Fewer than 10% of the CpG sites were methylated at the *Cd81*, *Ascl2*, *Kcnq1*-Intergenic1, *Ndn*, *Tssc4*, *Kcnq1*-Intergenic2, *Sfmbt2*, and *Cdkn1c* DMRs in mouse ES cells (Figure S7D). Therefore, it is difficult to assess if DNA methylation may be lost at these DMRs in the *Dnmt* or *Uhrf1* mutant ES cells.

In summary, DNMT3A and DNMT3B, together with DNMT1, maintained DNA methylation at the examined somatic DMRs in mouse ES cells. They appeared to play more important roles in maintaining DNA methylation at about half of the somatic DMRs than DNMT1. UHRF1 may not always work with DNMT1 in the maintenance of DNA methylation at the DMRs although they seemed to function similarly in most DMRs.

DNA methylation at the imprinting control regions in mouse embryonic stem cells after extended culture

Based on the COBRA and WGBS results of the mouse ES clones at P4, the earliest passage of ES cell culture we obtained for DNA methylation analysis, DNMT1 was the major DNA methyltransferase involved in the maintenance of DNA methylation at most known ICRs. Intriguingly, we found DNMT3A and DNMT3B, together with DNMT1, were also required for the maintenance of DNA methylation at a subset of known ICRs in mouse ES cells at P4. To test if the ES cell culture condition may cause DNA methylation to be lost at the ICRs, COBRA analysis was performed for some ICRs in two independent ES clones of *Dnmt1* KO, *Uhrf1* KO, *Dnmt3* DKO, *Dnmt* TKO as well as the WT control ES cells after they had been cultured on the feeder cells for a total of 10 passages (P10) and 20 passages (P20), respectively, as the last Lipofectamine-mediated transfection (see STAR Methods) (Figures S8 and S9).

Except for the slight change at the *Kcnq1ot1* ICR described later in discussion, there was no obvious difference in DNA methylation at the ICRs of the *Snrpn*, *Zac1*, *Peg1*, *Peg3*, *Peg13*, *H19*, IG-DMR of *Dlk1-Dio3* imprinted region, *Gpr1*, *Slc38a4*, *Peg5* and *Gnas1A* in the WT ES clones at P10 or P20 compared with those at P4 (Figures 3, S8, and S9). Similar to the COBRA results obtained from these *Dnmt* and *Uhrf1* mutant ES clones at P4 (Figure 3), DNA methylation was absent at the ICRs of the *Snrpn*, *Zac1*, *Peg1*, *Peg3*, and *Peg13* in the *Dnmt1* KO and *Uhrf1* KO mutant ES clones at P10 and P20, in comparison to the WT and *Dnmt* TKO ES clones at P10 and P20 (Figures S8 and S9). However, DNA methylation was still intact at these ICRs in the *Dnmt3* DKO mutant ES clones at P10 and P20 (Figures S8 and S9). Surprisingly, there seemed to be a slight increase in DNA methylation at the *Kcnq1ot1* ICR in all *Dnmt* and *Uhrf1* mutant ES clones as well as in the WT ES clones. Nevertheless, DNA methylation was still largely lost at the *Kcnq1ot1* ICR in the *Dnmt1* KO and *Uhrf1* KO mutant ES clones at P10 and P20, but mostly retained in the *Dnmt3* DKO mutant ES clones at P10 and P20, in comparison to the WT and *Dnmt* TKO ES clones at P10 and P20 (Figures S8 and S9). DNA methylation was lost at the *H19* ICR in the *Dnmt1* KO, *Uhrf1* KO and *Dnmt* TKO mutant ES clones at P10, whereas it was retained at the *H19* ICR in the *Dnmt3* DKO mutant ES clones at P10 (Figure S8). Similar results were obtained at the *H19* ICR in the *Dnmt1* KO, *Uhrf1* KO and *Dnmt3* DKO mutant ES clones at P20 (Figure S9). Intriguingly, *H19* ICR was slightly methylated in both *Dnmt* TKO mutant ES clones at P20 (Figure S9).

Similar to what had been observed at P4, DNA methylation was partially lost at the IG-DMR of the *Dlk1-Dio3* imprinted region as well as the ICRs of *Gpr1*, *Slc38a4*, *Peg5* and *Gnas1A* in the *Dnmt1* KO, *Uhrf1* KO, and *Dnmt3* DKO mutant ES clones at P10 and P20 (Figures 3, S8, and S9). Loss of DNA methylation seemed to be more severe at the IG-DMR and *Gpr1* ICR in two *Dnmt1* KO mutant ES clones at P4, P10, and P20 than in two *Dnmt3* DKO mutant ES clones at these passages, whereas there was a more severe loss of DNA methylation at the *Peg5* and *Gnas1A* ICRs in two *Dnmt3* DKO mutant ES clones at P4, P10 and P20 than in two *Dnmt1* KO mutant ES clones at the same passages (Figures 3, S8, and S9). Interestingly, there was still a residual amount of DNA methylation at IG-DMR, *Slc38a4*, *Peg5*, and *Gnas1A* ICRs in both *Dnmt* TKO mutant ES clones at P10 and P20 (Figures S8 and S9).

Taken together, DNA methylation was largely similar at the examined ICRs in the WT and mutant ES clones at P10 and P20 compared with those at P4. There was no further loss or significant gain of DNA methylation at the ICRs in the WT or *Dnmt1* KO or *Dnmt3* DKO mutant ES clones after the extended culture of ES cells. These results suggest that it is the maintenance DNA methylation, rather than *de novo* DNA methylation, that DNMT3A and DNMT3B play in regulating steady-state DNA methylation level at a subset of ICRs in mouse ES cells, which is functionally similar to DNMT1.

DISCUSSION

ZFP57 maintains DNA methylation at most known ICRs in mouse embryos (Jiang et al., 2021; Takahashi et al., 2015, 2019). It has been shown to maintain DNA methylation at multiple ICRs in our previous studies using the *Zfp57* mutant ES cells generated by homologous recombination or directly derived from the blastocysts (Lau et al., 2016a; Takikawa et al., 2013; Zuo et al., 2012). Similar findings were reported in other studies (Anvar et al., 2016; Coluccio et al., 2018; Quenneville et al., 2011; Riso et al., 2016). Consistent with the observed results in *Zfp57* maternal-zygotic mutant (M⁻Z⁻) embryos, we found DNA methylation was lost at most known ICRs in the mutant ES cells lacking ZFP57 (Figure 1) (Jiang et al., 2021; Li et al., 2008; Takahashi et al., 2019). Indeed, DNA methylation was similarly lost at multiple examined ICRs in the blastocyst-derived *Zfp57* mutant ES clones either from *Zfp57* zygotic mutant (M⁺Z⁻) embryos or *Zfp57* maternal-zygotic mutant embryos because maternal *Zfp57* was likely depleted in the *Zfp57* mutant ES clones derived from *Zfp57* zygotic mutant blastocysts (Lau et al., 2016a).

Although the loss of ZFP445 did not affect DNA methylation at most examined ICRs, DNA methylation at the *H19* ICR was significantly reduced in *Zfp57⁻/⁻*; *Zfp445⁻/⁻* mutant ES cells (Figure 1). These results are similar to what was reported in *Zfp445* zygotic mutant embryos as well as in the mutant embryos lacking both zygotic *Zfp57* and zygotic *Zfp445*, although there were no reported data for the *Zfp57* maternal-zygotic mutant embryos lacking zygotic *Zfp445* (Takahashi et al., 2019). Therefore, ZFP57 and ZFP445 may be partially redundant in maintaining DNA methylation at the *H19* ICR and this could be further examined in future research. It is unclear why DNA methylation at the *H19* ICR was somewhat increased in *Zfp445⁻/⁻* mutant ES cells (Figure 1).

There are a few previous studies suggesting the roles of TET proteins in genomic imprinting in mice (Dawlaty et al., 2013; Yamaguchi et al., 2013; Zhang et al., 2016). Except for the *H19* ICR, we did not observe a significant increase in DNA methylation at multiple ICRs examined in ES cells before (Liu et al., 2015). Nevertheless, we tested the functions of TET proteins again by removing *Zfp57* and *Zfp445* using CRISPR-Cas9 in the *Tet* TKO ES cells lacking all three TET proteins. DNA methylation at the examined ICRs including the *H19* ICR was still lost upon loss of ZFP57 and ZFP445 even in the absence of TET proteins (Figure 2). A similar loss of DNA methylation occurred to the ICRs in the *Tet* TKO ES cells upon loss of ZFP57, with the exception that there was only partial loss of DNA methylation at the *Peg13* ICR and no loss of DNA methylation was observed at the *H19* ICR in absence of both ZFP57 and TET proteins (Figure 2). These results further support the notion that ZFP57 is the master regulator in genomic imprinting in mouse ES cells and it may be partially redundant with ZFP445 at a small subset of the ICRs such as *H19* ICR. These also suggest that TET proteins may not be critical for stable maintenance of DNA methylation at the ICRs in mouse ES cells. We had proposed in a previous study that ZFP57 recruited DNA methyltransferases via KAP1/TRIM28 to maintain DNA methylation at the ICRs (Zuo et al., 2012). Therefore, ZFP57-mediated recruitment of DNA methyltransferases may be the key mechanism underlying the maintenance of ICR DNA methylation.

In this study, we found that DNMT1 is the primary DNA methyltransferase in maintaining DNA methylation at most known ICRs in mouse ES cells, whereas DNMT3A and DNMT3B contribute to the maintenance of DNA methylation at a subset of ICRs (Figures 4 and 7A). According to WGBS, DNMT3A and DNMT3B were required for maintaining DNA methylation at five ICRs including *Cdh15*, *Gpr1*, IG-DMR of the *Dlk1-Dio3* imprinted region, *H19*, and *Impact* although DNMT1 played much more important roles in maintaining DNA methylation at these five ICRs in mouse ES cells (Figure 4C). There was no obvious reduction in DNA methylation at the *H19* ICR in the *Dnmt3* DKO mutant ES clones at P4, P10, and P20 based on COBRA though (Figures 3, S8, and S9). This discrepancy could be owing to a small reduction in DNA methylation in the *Dnmt3* DKO mutant ES clones that were recognized by WGBS, but it could not be easily detected by COBRA that is based on gel analysis of the product after restriction enzyme digestion. In addition, only one CpG site of the *H19* ICR was analyzed by COBRA while many CpG sites were measured in WGBS, which may result in some difference if not all CpG sites of this ICR were uniform in DNA methylation level.

DNMT3A and DNMT3B were as equally important as DNMT1 in maintaining DNA methylation at four ICRs (*Slc38a4*, *Mcts2*, *Peg5*, and *Gnas1A*) with relatively low levels of DNA methylation in the WT ES clones (Figure 4D). Actually, they appeared to be more important than DNMT1 in the maintenance of DNA methylation at the *Peg5* and *Gnas1A* ICRs. Based on allelic DNA methylation analysis, DNMT3A and DNMT3B, together with DNMT1, maintained germline-derived DNA methylation imprint at a subset of ICRs in mouse ES cells (Figure 5) (Figure 7A). Therefore, DNMT3A and DNMT3B may be partially redundant with DNMT1 in maintaining DNA methylation at a subset of ICRs in mouse ES cells even though DNMT1 is the major DNA methyltransferase in maintaining DNA methylation at most known ICRs.

It is interesting that DNMT3A and DNMT3B seem to be more important than DNMT1 in maintaining DNA methylation at a few ICRs, particularly the ones with relatively low levels of DNA methylation (Figure 4D). This indicates that these ICRs are more sensitive to loss of DNA methylation in ES cells. DNMT1 is insufficient to maintain DNA methylation at these sensitive ICRs. In this case, DNMT3A and DNMT3B can provide an alternative pathway for maintaining DNA methylation at these ICRs in ES cells at relatively low levels. By contrast, DNA methylation at most ICRs is relatively stable in ES cells and DNMT1 is sufficient to maintain DNA methylation at these ICRs by itself without the need for DNMT3A and DNMT3B. Indeed, DNA methylation was found to be very stable in a subset of ICRs that was only lost after a very long-term passage of ES cells lacking DNMT3A and DNMT3B (Chen et al., 2003). After the extended culture for 10 and 20 passages, there was no significant loss of DNA methylation at the examined ICRs in the WT ES clones according to COBRA (Figures 3, S8, and S9). In general, similar loss of DNA methylation at the ICRs was obtained in the *Dnmt1* KO, *Dnmt3* DKO, and
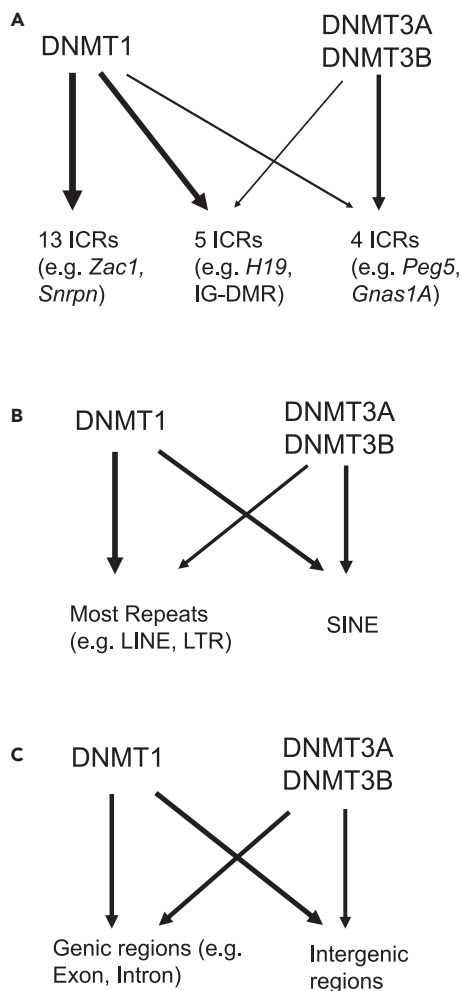
Figure 7. Schematic diagrams are shown for DNA methyltransferases in maintaining DNA methylation in mouse embryonic stem cells

The arrows mean that three DNMT proteins act at the maintenance methylation of the ICRs, repeats, genic or intergenic regions (A–C). The thickness of the lines of these arrows represents the importance of their maintenance functions, with thin or thick lines indicating minor or major roles, respectively.

(A) Maintenance of DNA methylation at ICRs in mouse ES cells. DNMT1 maintains DNA methylation at 13 ICRs such as *Zac1* and *Snrpn*. It is the major DNA methyltransferase that maintains DNA methylation at five other ICRs including *H19* and IG-DMR of the *Dlk1-Dio3* imprinted region. Interestingly, DNMT3A and DNMT3B contribute minor roles in the maintenance of DNA methylation at these five ICRs in mouse ES cells as well. In contrast, DNMT3A and DNMT3B, together with DNMT1, play major roles in maintaining DNA methylation at four ICRs including *Peg5* and *Gnas1A*.

(B) Maintenance of DNA methylation at repeats in mouse ES cells. DNMT1 is the major DNA methyltransferase that maintains DNA methylation at most repeats including LINE and LTR, whereas DNMT3A and DNMT3B are also important for the maintenance of DNA methylation at these repeats. By contrast, DNMT3A and DNMT3B play equally important roles as DNMT1 in maintaining DNA methylation at SINE.

(C) Maintenance of DNA methylation at genic and intergenic regions in mouse ES cells. DNMT3A and DNMT3B play equally important roles as DNMT1 in maintaining DNA methylation at the exons, introns, and other genic regions. DNMT1 appears to be the major DNA methyltransferase for maintaining DNA methylation in the intergenic regions although DNMT3A and DNMT3B are also important for the maintenance of DNA methylation in the intergenic regions.

Dnmt TKO mutant ES clones at P4, P10, and P20. These results support our hypothesis that DNMT3A and DNMT3B are involved in maintaining DNA methylation at a subset of ICRs including IG-DMR and a few other ICRs as the loss of DNMT1 did not result in further loss of DNA methylation at these ICRs even after the extended culture of the *Dnmt1* KO mutant ES clones. On the contrary, partial loss of DNA methylation persisted at these ICRs in the *Dnmt1* KO and *Dnmt3* DKO mutant ES clones at P10 and P20. *De novo* methylation mediated by DNMT3A and DNMT3B cannot compensate for partial loss of DNA methylation at these ICRs in the *Dnmt1* KO mutant ES cells. Therefore, three DNA methyltransferase are complementary in maintaining DNA methylation at a subset of ICRs, particularly those with relatively low levels of DNA methylation, although DNMT1 is essential for the maintenance of DNA methylation at most known ICRs in mouse ES cells.

DNMT1 is known to be mainly involved in the maintenance of DNA methylation, whereas DNMT3A and DNMT3B are *de novo* DNA methyltransferases (Li and Zhang, 2014). DNMT1 and UHRF1 were reported to function in *de novo* DNA methylation in oocytes (Li et al., 2018; Maenohara et al., 2017). DNMT1 can cooperate with DNMT3A in *de novo* methylation (Fatemi et al., 2002). There are a few other studies, suggesting that DNMT3A and DNMT3B may participate in the maintenance methylation of repetitive elements and genic regions in mouse ES cells (Chen et al., 2003; Gujar et al., 2019; Liang et al., 2002). Consistent with these studies, DNMT3A and DNMT3B were as important as DNMT1 in maintaining DNA methylation at all repeats, most DMRs, and other genomic regions in mouse ES cells (Figures 7, S6, and S7). They were required for maintenance of DNA methylation not only at the promoters and CGIs with relatively low levels of DNA methylation but also in the highly methylated repeats, DMRs, gene bodies, and intergenic regions. Thus, three DNA methyltransferases are all required but they are partially redundant for maintaining DNA methylation at the repeats, DMRs, and other genomic regions in mouse ES cells.

Limitations of the study

Most of the deletion mutant ES clones were generated by CRISPR from the 129/DBA hybrid wild-type ES clone D1911 (Lau et al., 2016b). However, *Tet* TKO mutant ES clone was used for the generation of *Zfp57* and/or *Zfp445* deletion mutations to examine if loss of three TET proteins could prevent loss of DNA methylation at the ICRs of the imprinted regions caused by loss of ZFP57 and ZFP445 in the ES cells (Hu et al., 2014). DNA methylation at the *Peg13* ICR was partially lost in two *Zfp57* deletion mutant ES clones derived from the *Tet* TKO ES cell line, whereas it was completely lost in two *Zfp57* KO ES clones generated from D1911 (Figures 1 and 2). DNA methylation at the *H19* ICR appeared to be slightly different when both ZFP57 and ZFP445 were lost in the DKO mutant ES clones derived from these two different ES cell lines. DNA methylation at other examined ICRs was similarly affected in these mutant ES clones (Figures 1 and 2). We suspect that small differences observed at the *Peg13* and *H19* ICRs could be owing to some inherent differences of two parental ES cell lines. This hypothesis may be tested in the future when the same ES cell line is used for the generation of *Zfp57* and *Zfp445* deletion mutations with or without TET proteins.

There are quite many SNPs that are present in the 129/DBA hybrid wild-type ES clone D1911 derived from the mating of a female mouse on the 129S6/SvEvTac genetic background and a male mouse on the DBA2/J genetic background. But only a subset of ICRs harbors an SNP that has allowed us to perform allelic analysis of DNA methylation at these ICRs in the WGBS analysis. Therefore, it is not possible to determine how germline-derived DNA methylation was lost at the *H19*, *Peg5*, and other ICRs in the absence of DNMT proteins, unlike a subset of ICRs such as *Gnas1A* and *Impact* in this study (Figure 6). In the future, a hybrid ES clone carrying more SNPs may be required to examine allelic DNA methylation at most ICRs upon loss of DNMT proteins.

STAR★METHODS

Detailed methods are provided in the online version of this paper and include the following:

- KEY RESOURCES TABLE
- RESOURCE AVAILABILITY
  - Lead contact
  - Material availability
  - Data and code availability
- EXPERIMENTAL MODEL AND SUBJECT DETAILS
  - ES cell lines
- METHODS DETAILS
  - Construction of sgRNA-expressing plasmids for generating deletion mutations by CRISPR-Cas9
  - ES cell culture
  - Obtaining deletion mutant ES clones by CRISPR-Cas9
  - Western blot analysis
  - Immunofluorescence of ES cells
  - Genomic DNA sample preparation
  - COBRA analysis of the ICRs in ES cells
  - Whole-genome bisulfite sequencing (WGBS) of ES samples
  - Generation of the SNP data for the 129/DBA hybrid ES cells
  - Assignment of allelic DNA methylation reads
- QUANTIFICATION AND STATISTICAL ANALYSIS

SUPPLEMENTAL INFORMATION

Supplemental information can be found online at https://doi.org/10.1016/j.isci.2022.105003.

and Multi-Omics Core Facility (MOCF) at the School of Life Science and Technology in ShanghaiTech University for providing technical support.

AUTHOR CONTRIBUTIONS

X.L. conceived and designed the study, wrote the article with the help of all authors. Y.L., Z.X, J.S., Y.Z., S.Y., Q.C., C.S., S.G., and Q. L. performed all experiments for this study. Z.X. and Y.Z. carried out WGS and WGBS sequence data analysis.

DECLARATION OF INTERESTS

The authors declare no competing interests.

REFERENCES

Anvar, Z., Cammisa, M., Riso, V., Baglivo, I., Kukreja, H., Sparago, A., Girardot, M., Lad, S., De Feis, I., Cerrato, F., et al. (2016). ZFP57 recognizes multiple and closely spaced sequence motif variants to maintain repressive epigenetic marks in mouse embryonic stem cells. Nucleic Acids Res. *44*, 1118–1132. https://doi.org/10.1093/nar/gkv1059.

Bar, S., and Benvenisty, N. (2019). Epigenetic aberrations in human pluripotent stem cells. EMBO J. *38*, e101033. https://doi.org/10.15252/embj.2018101033.

Bar, S., and Benvenisty, N. (2020). Human pluripotent stem cells: derivation and applications. Nat. Rev. Mol. Cell Biol. https://doi.org/10.1038/s41580-020-00309-7.

Barlow, D.P., and Bartolomei, M.S. (2014). Genomic imprinting in mammals. Cold Spring Harb. Perspect. Biol. *6*, a018382. https://doi.org/10.1101/cshperspect.a018382.

Bartolomei, M.S., Oakey, R.J., and Wutz, A. (2020). Genomic imprinting: an epigenetic regulatory system. PLoS Genet. *16*, e1008970. https://doi.org/10.1371/journal.pgen.1008970.

Bochtler, M., Kolano, A., and Xu, G.L. (2017). DNA demethylation pathways: additional players and regulators. Bioessays *39*, 1–13. https://doi.org/10.1002/bies.201600178.

Chen, T., Ueda, Y., Dodge, J.E., Wang, Z., and Li, E. (2003). Establishment and maintenance of genomic methylation patterns in mouse embryonic stem cells by Dnmt3a and Dnmt3b. Mol. Cell Biol. *23*, 5594–5605. https://doi.org/10.1128/MCB.23.16.5594-5605.2003.

Chen, Z., and Zhang, Y. (2020). Role of mammalian DNA methyltransferases in development. Annu. Rev. Biochem. *89*, 135–158. https://doi.org/10.1146/annurev-biochem-103019-102815.

Coluccio, A., Ecco, G., Duc, J., Offner, S., Turelli, P., and Trono, D. (2018). Individual retrotransposon integrants are differentially controlled by KZFP/KAP1-dependent histone methylation, DNA methylation and TET-mediated hydroxymethylation in naive embryonic stem cells. Epigenet. Chromatin *11*, 7. https://doi.org/10.1186/s13072-018-0177-1.

Dawlaty, M.M., Breiling, A., Le, T., Raddatz, G., Barrasa, M.I., Cheng, A.W., Gao, Q., Powell, B.E., Li, Z., Xu, M., et al. (2013). Combined deficiency of Tet1 and Tet2 causes epigenetic abnormalities but is compatible with postnatal development. Dev. Cell *24*, 310–323. https://doi.org/10.1016/j.devcel.2012.12.015.

Fatemi, M., Hermann, A., Gowher, H., and Jeltsch, A. (2002). Dnmt3a and Dnmt1 functionally cooperate during de novo methylation of DNA. Eur. J. Biochem. *269*, 4981–4984. https://doi.org/10.1046/j.1432-1033.2002.03198.x.

Ge, Y.Z., Pu, M.T., Gowher, H., Wu, H.P., Ding, J.P., Jeltsch, A., and Xu, G.L. (2004). Chromatin targeting of de novo DNA methyltransferases by the PWWP domain. J. Biol. Chem. *279*, 25447–25454. https://doi.org/10.1074/jbc.M312296200.

Gujar, H., Weisenberger, D.J., and Liang, G. (2019). The roles of human DNA methyltransferases and their isoforms in shaping the epigenome. Genes *10*, E172. https://doi.org/10.3390/genes10020172.

Hirasawa, R., and Feil, R. (2008). A KRAB domain zinc finger protein in imprinting and disease. Dev. Cell *15*, 487–488. https://doi.org/10.1016/j.devcel.2008.09.006.

Hu, X., Zhang, L., Mao, S.Q., Li, Z., Chen, J., Zhang, R.R., Wu, H.P., Gao, J., Guo, F., Liu, W., et al. (2014). Tet and TDG mediate DNA demethylation essential for mesenchymal-to-epithelial transition in somatic cell reprogramming. Cell Stem Cell *14*, 512–522. https://doi.org/10.1016/j.stem.2014.01.001.

Jiang, W., Shi, J., Zhao, J., Wang, Q., Cong, D., Chen, F., Zhang, Y., Liu, Y., Zhao, J., Chen, Q., et al. (2021). ZFP57 dictates allelic expression switch of target imprinted genes. Proc. Natl. Acad. Sci. USA *118*. e2005377118. https://doi.org/10.1073/pnas.2005377118.

Juan, A.M., and Bartolomei, M.S. (2019). Evolving imprinting control regions: KRAB zinc fingers hold the key. Genes Dev. *33*, 1–3. https://doi.org/10.1101/gad.322990.118.

Khamlichi, A.A., and Feil, R. (2018). Parallels between mammalian mechanisms of monoallelic gene expression. Trends Genet. *34*, 954–971. https://doi.org/10.1016/j.tig.2018.08.005.

Krueger, F., and Andrews, S.R. (2011). Bismark: a flexible aligner and methylation caller for Bisulfite-Seq applications. Bioinformatics *27*, 1571–1572. https://doi.org/10.1093/bioinformatics/btr167.

Krueger, F., and Andrews, S.R. (2016). SNPsplit: allele-specific splitting of alignments between genomes with known SNP genotypes. F1000Res. *5*, 1479. https://doi.org/10.12688/f1000research.9037.2.

Lau, H.T., Liu, L., and Li, X. (2016a). Zfp57 mutant ES cell lines directly derived from blastocysts. Stem Cell Res. *16*, 282–286. https://doi.org/10.1016/j.scr.2015.12.038.

Lau, H.T., Liu, L., Ray, C., Bell, F.T., and Li, X. (2016b). Derivation of hybrid ES cell lines from two different strains of mice. Stem Cell Res. *16*, 252–255.

Li, E., and Zhang, Y. (2014). DNA methylation in mammals. Cold Spring Harb. Perspect. Biol. *6*, a019133. https://doi.org/10.1101/cshperspect.a019133.

Li, H., and Durbin, R. (2009). Fast and accurate short read alignment with Burrows-Wheeler transform. Bioinformatics *25*, 1754–1760. https://doi.org/10.1093/bioinformatics/btp324.

Li, M.J., and Li, X. (2020). Three paternally imprinted regions are sequentially required in prenatal and postnatal mouse development. Sci. China Life Sci. *63*, 165–168. https://doi.org/10.1007/s11427-019-1561-1.

Li, Q., Li, Y., Yin, Q., Huang, S., Wang, K., Zhuo, L., Li, W., Chang, B., and Li, J. (2020). Temporal regulation of prenatal embryonic development by paternal imprinted loci. Sci. China Life Sci. *63*, 1–17. https://doi.org/10.1007/s11427-019-9817-6.

Li, X. (2013). Genomic imprinting is a parental effect established in mammalian germ cells. Curr. Top. Dev. Biol. *102*, 35–59. https://doi.org/10.1016/B978-0-12-416024-8.00002-7.

Li, X., Ito, M., Zhou, F., Youngson, N., Zuo, X., Leder, P., and Ferguson-Smith, A.C. (2008). A maternal-zygotic effect gene, Zfp57, maintains both maternal and paternal imprints. Dev. Cell 15, 547–557. https://doi.org/10.1016/j.devcel.2008.08.014.

Li, X., Li, M.J., Yang, Y., and Bai, Y. (2019b). Effects of reprogramming on genomic imprinting and the application of pluripotent stem cells. Stem Cell Res. 41, 101655. https://doi.org/10.1016/j.scr.2019.101655.

Li, Y., Zhang, Z., Chen, J., Liu, W., Lai, W., Liu, B., Li, X., Liu, L., Xu, S., Dong, Q., et al. (2018). Stella safeguards the oocyte methylome by preventing de novo methylation mediated by DNMT1. Nature 564, 136–140. https://doi.org/10.1038/s41586-018-0751-5.

Liang, G., Chan, M.F., Tomigahara, Y., Tsai, Y.C., Gonzales, F.A., Li, E., Laird, P.W., and Jones, P.A. (2002). Cooperativity between DNA methyltransferases in the maintenance methylation of repetitive elements. Mol. Cell Biol. 22, 480–491. https://doi.org/10.1128/MCB.22.2.480-491.2002.

Liu, L., Mao, S.Q., Ray, C., Zhang, Y., Bell, F.T., Ng, S.F., Xu, G.L., and Li, X. (2015). Differential regulation of genomic imprinting by TET proteins in embryonic stem cells. Stem Cell Res. 15, 435–443. https://doi.org/10.1016/j.scr.2015.08.010.

Liu, Y., Chen, Q., Song, C., Xu, Z., Yang, S., and Li, X. (2022). Efficient isolation of mouse deletion mutant embryonic stem cells by CRISPR. STAR Protoc. 3, 101436. https://doi.org/10.1016/j.xpro.2022.101436.

Liu, Y., Olanrewaju, Y.O., Zhang, X., and Cheng, X. (2013). DNA recognition of 5-carboxylcytosine by a Zfp57 mutant at an atomic resolution of 0.97 A. Biochemistry 52, 9310–9317. https://doi.org/10.1021/bi401360n.

Liu, Y., Toh, H., Sasaki, H., Zhang, X., and Cheng, X. (2012). An atomic model of Zfp57 recognition of CpG methylation within a specific DNA sequence. Genes Dev. 26, 2374–2379. https://doi.org/10.1101/gad.202200.112.

Mackay, D.J.G., Callaway, J.L.A., Marks, S.M., White, H.E., Acerini, C.L., Boonen, S.E., Dayanikli, P., Firth, H.V., Goodship, J.A., Haemers, A.P., et al. (2008). Hypomethylation of multiple imprinted loci in individuals with transient neonatal diabetes is associated with mutations in ZFP57. Nat. Genet. 40, 949–951. https://doi.org/10.1038/ng.187.

Maenohara, S., Unoki, M., Toh, H., Ohishi, H., Sharif, J., Koseki, H., and Sasaki, H. (2017). Role of UHRF1 in de novo DNA methylation in oocytes and maintenance methylation in preimplantation embryos. PLoS Genet. 13, e1007042. https://doi.org/10.1371/journal.pgen.1007042.

Mancini, M., Magnani, E., Macchi, F., and Bonapace, I.M. (2021). The multi-functionality of UHRF1: epigenome maintenance and preservation of genome integrity. Nucleic Acids

Res. 49, 6053–6068. https://doi.org/10.1093/nar/gkab293.

McKenna, A., Hanna, M., Banks, E., Sivachenko, A., Cibulskis, K., Kernytsky, A., Garimella, K., Altshuler, D., Gabriel, S., Daly, M., and DePristo, M.A. (2010). The Genome Analysis Toolkit: a MapReduce framework for analyzing next-generation DNA sequencing data. Genome Res. 20, 1297–1303. https://doi.org/10.1101/gr.107524.110.

Monk, D., Mackay, D.J.G., Eggermann, T., Maher, E.R., and Riccio, A. (2019). Genomic imprinting disorders: lessons on how genome, epigenome and environment interact. Nat. Rev. Genet. 20, 235–248. https://doi.org/10.1038/s41576-018-0092-0.

Quenneville, S., Verde, G., Corsinotti, A., Kapopoulou, A., Jakobsson, J., Offner, S., Baglivo, I., Pedone, P.V., Grimaldi, G., Riccio, A., and Trono, D. (2011). In embryonic stem cells, ZFP57/KAP1 recognize a methylated hexanucleotide to affect chromatin and DNA methylation of imprinting control regions. Mol. Cell 44, 361–372. https://doi.org/10.1016/j.molcel.2011.08.032.

Quinlan, A.R., and Hall, I.M. (2010). BEDTools: a flexible suite of utilities for comparing genomic features. Bioinformatics 26, 841–842. https://doi.org/10.1093/bioinformatics/btq033.

Riso, V., Cammisa, M., Kukreja, H., Anvar, Z., Verde, G., Sparago, A., Acurzio, B., Lad, S., Lonardo, E., Sankar, A., et al. (2016). ZFP57 maintains the parent-of-origin-specific expression of the imprinted genes and differentially affects non-imprinted targets in mouse embryonic stem cells. Nucleic Acids Res. 44, 8165–8178. https://doi.org/10.1093/nar/gkw505.

Strogantsev, R., Krueger, F., Yamazawa, K., Shi, H., Gould, P., Goldman-Roberts, M., McEwen, K., Sun, B., Pedersen, R., and Ferguson-Smith, A.C. (2015). Allele-specific binding of ZFP57 in the epigenetic regulation of imprinted and non-imprinted monoallelic expression. Genome Biol. 16, 112. https://doi.org/10.1186/s13059-015-0672-7.

Takahashi, N., Coluccio, A., Thorball, C.W., Planet, E., Shi, H., Offner, S., Turelli, P., Imbeault, M., Ferguson-Smith, A.C., and Trono, D. (2019). ZNF445 is a primary regulator of genomic imprinting. Genes Dev. 33, 49–54. https://doi.org/10.1101/gad.320069.118.

Takahashi, N., Gray, D., Strogantsev, R., Noon, A., Delahaye, C., Skarnes, W.C., Tate, P.H., and Ferguson-Smith, A.C. (2015). ZFP57 and the targeted maintenance of postfertilization genomic imprints. Cold Spring Harb. Symp. Quant. Biol. 80, 177–187. https://doi.org/10.1101/sqb.2015.80.027466.

Takikawa, S., Wang, X., Ray, C., Vakulenko, M., Bell, F.T., and Li, X. (2013). Human and mouse ZFP57 proteins are functionally interchangeable in maintaining genomic imprinting at multiple imprinted regions in mouse ES cells. Epigenetics 8, 1268–1279.

Tucci, V., Isles, A.R., Kelsey, G., and Ferguson-Smith, A.C.; Erice Imprinting Group (2019). Genomic imprinting and physiological processes in mammals. Cell 176, 952–965. https://doi.org/10.1016/j.cell.2019.01.043.

Van der Auwera, G.A., Carneiro, M.O., Hartl, C., Poplin, R., Del Angel, G., Levy-Moonshine, A., Jordan, T., Shakir, K., Roazen, D., Thibault, J., et al. (2013). From FastQ data to high confidence variant calls: the Genome Analysis Toolkit best practices pipeline. Curr. Protoc. Bioinformatics 43, 11.10.1–11.10.33. https://doi.org/10.1002/0471250953.bi1110s43.

Wang, Q., Yu, G., Ming, X., Xia, W., Xu, X., Zhang, Y., Zhang, W., Li, Y., Huang, C., Xie, H., et al. (2020). Imprecise DNMT1 activity coupled with neighbor-guided correction enables robust yet flexible epigenetic inheritance. Nat. Genet. 52, 828–839. https://doi.org/10.1038/s41588-020-0661-y.

Wu, H., and Zhang, Y. (2014). Reversing DNA methylation: mechanisms, genomics, and biological functions. Cell 156, 45–68. https://doi.org/10.1016/j.cell.2013.12.019.

Wu, X., and Zhang, Y. (2017). TET-mediated active DNA demethylation: mechanism, function and beyond. Nat. Rev. Genet. 18, 517–534. https://doi.org/10.1038/nrg.2017.33.

Xu, G.L., and Bochtler, M. (2020). Reversal of nucleobase methylation by dioxygenases. Nat. Chem. Biol. 16, 1160–1169. https://doi.org/10.1038/s41589-020-00675-5.

Yamaguchi, S., Shen, L., Liu, Y., Sendler, D., and Zhang, Y. (2013). Role of Tet1 in erasure of genomic imprinting. Nature 504, 460–464. https://doi.org/10.1038/nature12805.

Zeng, Y., and Chen, T. (2019). DNA methylation reprogramming during mammalian development. Genes 10, E257. https://doi.org/10.3390/genes10040257.

Zhang, H., Gao, Q., Tan, S., You, J., Lyu, C., Zhang, Y., Han, M., Chen, Z., Li, J., Wang, H., et al. (2019). SET8 prevents excessive DNA methylation by methylation-mediated degradation of UHRF1 and DNMT1. Nucleic Acids Res. 47, 9053–9068. https://doi.org/10.1093/nar/gkz626.

Zhang, W., Xia, W., Wang, Q., Towers, A.J., Chen, J., Gao, R., Zhang, Y., Yen, C.A., Lee, A.Y., Li, Y., et al. (2016). Isoform switch of TET1 regulates DNA demethylation and mouse development. Mol. Cell 64, 1062–1073. https://doi.org/10.1016/j.molcel.2016.10.030.

Zuo, X., Sheng, J., Lau, H.T., McDonald, C.M., Andrade, M., Cullen, D.E., Bell, F.T., Iacovino, M., Kyba, M., Xu, G., and Li, X. (2012). Zinc finger protein ZFP57 requires its co-factor to recruit DNA methyltransferases and maintains DNA methylation imprint in embryonic stem cells via its transcriptional repression domain. J. Biol. Chem. 287, 2107–2118. https://doi.org/10.1074/jbc.M111.322644.

STAR★METHODS

KEY RESOURCES TABLE

REAGENT or RESOURCE	SOURCE	IDENTIFIER
Antibodies		
Rabbit polyclonal anti-UHRF1	Santa Cruz, USA	Cat. # SC-98817; RRID: AB_2214278
Mouse monoclonal anti-DNMT1	Abcam, USA	Cat. # ab13537; RRID: AB_300438
Rabbit polyclonal anti-DNMT3A	Abcam, USA	Cat. # ab2850; RRID: AB_303355
Mouse monoclonal anti-DNMT3B	Xu Lab, Chinese Academy of Sciences	(Ge et al., 2004)
Rabbit polyclonal anti-ZFP57	Li Lab, ShanghaiTech University	(Li et al., 2008)
Bacterial and virus strains		
T1 competent cells	Shanghai Weidi Biotechnology Co, Ltd	Cat. # DL1015S
Chemicals, peptides, and recombinant proteins		
Fetal bovine serum (FBS)	Sigma, USA	Cat. #F2442
Pennicillin/Streptomycin solution	Beyotime, China	Cat. #C0222
Trypsin-EDTA solution	Sigma, USA	Cat. #T4049
Leukemia inhibitory factor (LIF) or ESGRO	Millipore, USA	Cat. # ESG1107
T4 DNA ligase	Takara, Japan	Cat. # 2011A
T4 polynucleotide kinase (PNK) (10 U/μL)	Takara, Japan	Cat. # 2021S
*Bpi*I	Thermo Scientific, USA	Cat. # FD1014
Gelatin	Sinopharm Chemical Reagent (SCR), China	Cat. # 9000-70-8
Bacto-yeast extract	Sangon, China	Cat. # A515245-0500
Bacto-tryptone	Sangon, China	Cat. # A505247-0500
Agar	Macklin, China	Cat. # A800730
Lipofectamine 2000	Invitrogen, USA	Cat. # 11668019
DMEM	Invitrogen, USA	Cat. #C11995500CP
Non-essential amino acid (NEAA) solution (100X)	Hyclone, USA	Cat. # SH30238.01
Dithiothreitol (DTT)	Fisher Biotech, USA	Cat. # BP172-25
Dimethyl sulfoxide (DMSO)	Amethyst, China	Cat. # 966629
Carbenicillin	Yeasen, China	Cat. # 60202ES08
β-mercaptoethanol	Sigma, USA	Cat. #M3148
Sodium chloride (NaCl)	Sangon, China	Cat. # A501218-0001
PBS (20X)	Sangon, China	Cat. #B548117-0500
Proteinase K	Abcone, China	Cat. #P78893
Tris	Beyotime Biotechnology, China	Cat. # ST761
SDS	Sigma, USA	Cat. #L4390
Agarose	Abcone, China	Cat. # A88490
100bp Plus DNA Ladder	Monad, China	Cat. # ME40101M
PageRular Prestained Protein Ladder	Fermentas, USA	Cat. # 26617
GeneGreen nucleic acid dye	Tiangen, China	Cat. # RT210
EDTA	Amethyst,China	Cat. # 976151-500G
*Eco*RV	NEB, USA	Cat. #R0195S
*Hin*dIII	NEB, USA	Cat. #R0104S
*Taq*I	Monad, China	Cat. # MF02801S
*Cla*I	Monad, China	Cat. # MF00501M

Continued

REAGENT or RESOURCE	SOURCE	IDENTIFIER
*Hha*I	NEB, USA	Cat. #R0139V
*Bst*UI	NEB, USA	Cat. #R0518L
Critical commercial assays		
AxyPrep DNA Gel Extraction Kit	Axygen of Corning	Cat. # 35717KE1
AxyPrep Endo-Free Plasmid Midiprep Kit	Axygen of Corning	Cat. # 09318KA2
EZ DNA Methylation-Gold™ Kit	ZYMO Research, USA	Cat. #D5006
Blood/Cell/Tissue Genomic DNA Extract Kit	TIANGEN, China	Cat. # DP304-02
Deposited data		
Raw and analyzed WGBS Data and WGS data	This paper	GEO: GSE208759
Experimental models: Cell lines		
D1911	Li Lab, ShanghaiTech	(Lau et al., 2016b)
Tet TKO	Xu Lab, Chinese Academy of Sciences	(Hu et al., 2014)
Oligonucleotides		
CACCGAATAGGAATTTGTGACGTCC	Genewiz	*Zfp445*-sgRNA1-F
AAACGGACGTCACAAATTCCTATTC	Genewiz	*Zfp445*-sgRNA1-R
CACCGAGCTCAGCGCAATCTTTATC	Genewiz	*Zfp445*-sgRNA2-F
AAACGATAAAGATTGCGCTGAGCTC	Genewiz	*Zfp445*-sgRNA2-R
CACCGTGACAATATCTTCGGTGCA	Genewiz	*Uhrf1*-sgRNA1-F
AAACTGCACCGAAGATATTGTCAC	Genewiz	*Uhrf1*-sgRNA1-R
CACCGTGAGCTATACGGCAACATC	Genewiz	*Uhrf1*-sgRNA2-F
AAACGATGTTGCCGTATAGCTCAC	Genewiz	*Uhrf1*-sgRNA2-R
CACCGCTAAATGAGCACGTCGGTGA	Genewiz	*Zfp57*-sgRNA1-F
AAACTCACCGACGTGCTCATTTAGC	Genewiz	*Zfp57*-sgRNA1-R
CACCGATACTTGAGGGCGGGCGCTT	Genewiz	*Zfp57*-sgRNA2-F
AAACAAGCGCCCGCCCTCAAGTATC	Genewiz	*Zfp57*-sgRNA2-R
CACCGATCACGGCTCACTTCACGAA	Genewiz	*Dnmt1*-sgRNA1-F
AAACTTCGTGAAGTGAGCCGTGATC	Genewiz	*Dnmt1*-sgRNA1-R
CACCGCCAACGGTTGTCCCGCCAA	Genewiz	*Dnmt1*-sgRNA2-F
AAACTTGGCGGGACAACCGTTGGC	Genewiz	*Dnmt1*-sgRNA2-R
CACCGTAGATGGCTTTGCGGTACAT	Genewiz	*Dnmt3a*-sgRNA1-F
AAACATGTACCGCAAAGCCATCTAC	Genewiz	*Dnmt3a*-sgRNA1-R
CACCGTTCCAGCCCTCGGGTCCTAA	Genewiz	*Dnmt3a*-sgRNA2-F
AAACTTAGGACCCGAGGGCTGGAAC	Genewiz	*Dnmt3a* -sgRNA2-R
CACCGAACGTCAATCCTGCCCGCAA	Genewiz	*Dnmt3b*-sgRNA1-F
AAACTTGCGGGCAGGATTGACGTTC	Genewiz	*Dnmt3b*-sgRNA1-R
CACCGATTGCTGGGTACAACTTGGG	Genewiz	*Dnmt3b*-sgRNA2-F
AAACCCCAAGTTGTACCCAGCAATC	Genewiz	*Dnmt3b*-sgRNA2-R
AGTGCGTCCTTCGTTACCTG	Genewiz	*Zfp445*-F1
GTGAAGGTAGCTGGGGATAC	Genewiz	*Zfp445*-R1
GGACCTACAAGCAAGCAGAC	Genewiz	*Zfp445*-F2
CAGGGGTATTCAAAGGTGGAC	Genewiz	*Zfp57*-F1
CGGACCACTGTAATAGAGTTGG	Genewiz	*Zfp57*-R1
CATCAGAGCAGAGGTCTCTTGC	Genewiz	*Uhrf1*-F1
GGCTGGGCTCCTAGCACTAG	Genewiz	*Uhrf1*-R1

Continued

REAGENT or RESOURCE	SOURCE	IDENTIFIER
GGTTGGACCTTTGCTTGCAGC	Genewiz	*Uhrf1*-R2
GGTGGTCACTGTAAACCGT	Genewiz	*Dnmt1*-F1
CCTGCCTAAAACCCCTGATGA	Genewiz	*Dnmt1*-R1
CAGTTGTGTGACTTGGAAACC	Genewiz	*Dnmt1*-F2
GTCAGAAGGCACTTGGCTTAC	Genewiz	*Dnmt3a*-F1
GGATCCCTGGACGTCGGAG	Genewiz	*Dnmt3a*-R1
GCACCAGGAAAGCAGATGAC	Genewiz	*Dnmt3a*-F2
GTCTCATGCTGTCCCCATCC	Genewiz	*Dnmt3b*-F1
ACATAAGCCCAAGAGTAGCA	Genewiz	*Dnmt3b*-R1
GCCTGTGTCAAACACGTTCTC	Genewiz	*Dnmt3b*-F2
Recombinant DNA		
pX330	Addgene, USA	42230
Software and algorithms		
Bismark	Krueger and Andrews (2011)	https://www.bioinformatics.babraham.ac.uk/projects/bismark/
BedTools	Quinlan and Hall (2010)	https://bedtools.readthedocs.io/en/latest/
Trim Galore	Babraham Institute	https://www.bioinformatics.babraham.ac.uk/projects/trim_galore/
SNPsplit	Krueger and Andrews (2016).	https://www.bioinformatics.babraham.ac.uk/projects/SNPsplit/
Burrows-Wheeler Aligner (BWA)	Li and Durbin (2009)	http://bio-bwa.sourceforge.net/index.shtml
GATK	McKenna et al. (2010); Van der Auwera et al. (2013)	https://gatk.broadinstitute.org
Others		
Original code	N/A	N/A

RESOURCE AVAILABILITY

Lead contact

Further information and requests for resources and reagents should be directed to and will be fulfilled by the lead contact, Dr. Xiajun Li (lixj1@shanghaitech.edu.cn)

Material availability

All ES cell clones generated in this study are available with a completed Material Transfer Agreement upon request directed to the lead contact.

Data and code availability

- The WGBS data for the mouse ES clones used in this study have been deposited in the Gene Expression Omnibus (GEO). They can be accessed under the GEO number GSE208759. The WGS data for two 129S6/SvEvTac genomic DNA samples can also be accessed under the GEO number GSE208759.

- There is no original code developed in this study.

- Any additional information that is required to analyze the data reported in this paper is available from the lead contact upon request.

EXPERIMENTAL MODEL AND SUBJECT DETAILS

ES cell lines

The 129/DBA hybrid D1911 ES cell line was derived from the blastocyst in a previous study of our lab, which was generated from the mating between a female mouse on the 129S6/SvEvTac genetic background and a male mouse on the DBA2/J genetic background (Lau et al., 2016b). The *Tet* TKO ES cell line containing

mutations in *Tet1*, *Tet2* and *Tet3* was generated in another study (Hu et al., 2014). These ES cell lines and their derived mutant ES clones were cultured on the irradiated SNL feeder cells with the ES cell growth medium containing 15% of heat inactivated fetal bovine serum (FBS) (Liu et al., 2022). They were frozen in liquid nitrogen for long-term storage in the freezing medium containing 25% FBS and 10% of dimethyl sulfoxide (DMSO). When they were needed again, the frozen ES clones were thawed in the water bath of 37°C and plated onto the SNL feeder cells after DMSO was washed away from the thawed ES cells with 5–10 mL of ES cell growth medium in a 15-mL conical tube (Liu et al., 2022).

METHODS DETAILS

Construction of sgRNA-expressing plasmids for generating deletion mutations by CRISPR-Cas9

Standard molecular cloning procedures were used to make the CRISPR-Cas9 sgRNA plasmid constructs targeting mouse *Zfp57*, *Zfp445*, *Uhrf1*, *Dnmt1*, *Dnmt3a* and *Dnmt3b* genes (Liu et al., 2022). Two complementary oligos for each sgRNA were annealed *in vitro* and cloned into pX330 with restriction enzyme digestion and ligation (Table S1). The resultant plasmids were sequenced to confirm the inserted DNA fragment encoding the sgRNA targeting the gene of the interest.

ES cell culture

Standard ES cell culture protocol was used for this study (Liu et al., 2022). The ES cell growth medium contained DMEM with glutamine and high glucose and 15% of heat inactivated fetal bovine serum (FBS), plus non-essential amino acids and β-mercaptoethanol. The cell culture plates were seeded with irradiated mouse embryonic fibroblast (MEF) or SNL feeder cells first before the resuspended ES cells were plated on top of the feeder cells. The medium was changed daily when there were enough ES cells growing to prevent spontaneous differentiation of ES cells. Then the ES cell culture was harvested by trypsin digestion and split again before it was too confluent. They were frozen in the freezing medium containing 25% FBS and 10% of DMSO for long-term storage until they were needed again.

Obtaining deletion mutant ES clones by CRISPR-Cas9

An CRISPR-based approach developed in our lab was used to generate deletion mutant ES clones (Liu et al., 2022). First, D1911 ES cells were plated on the feeder cells made of the MEF cells derived from the mice expressing the puromycin-resistant gene. Then two pX330 constructs containing the inserted DNA fragment encoding the sgRNAs targeting the gene of interest were mixed in order to generate a deletion mutation for all mutant ES clones except for generation of the *Zfp57* mutations in the *Tet* TKO ES cells (Table S2) (see below). This plasmid DNA mix was co-transfected with the plasmid expressing puromycin-resistant gene product into D1911 ES cells by Lipofectamine 2000. The transfected ES cells were subjected to 1 μg/mL of puromycin selection for 2 days starting the day after transfection. Then the transfected ES cells were grown with regular ES cell growth medium until the ES cell colonies were large enough for picking individually. The picked ES cell colonies were digested with trypsin and plated onto a well of 24-well plate seeded with the SNL feeder cells. Genomic DNA samples derived from these picked ES clones were used for PCR-based screening and sequencing to identify the candidate ES clones containing deletion at the target gene. The PCR product spanning the deletion of the target gene was cloned into the pBluescript vector by restriction digestion and ligation, and the ligation mixture was transformed into competent bacterial cells afterwards. The resultant bacterial colonies were subjected to sequencing to identify the exact deleted region on the target gene. The mutant ES clones containing the deletion mutation that likely resulted in a null mutation of the target gene were cultured again to obtain the protein lysate samples for western blot and genomic DNA samples for DNA methylation analysis, respectively.

The control WT ES clones were similarly picked from the growing ES cell culture after D1911 ES cells were subjected to the same Lipofectamine-mediated transfection experiment with the plasmid containing puromycin-resistant gene and the empty pX330 plasmid without expressing any sgRNA, which was also followed by 1 μg/mL of puromycin selection for 2 days. The mutant ES clones of *Zfp57*$^{-/-}$ and *Zfp445*$^{-/-}$ were generated by CRISPR-Cas9 through Lipofectamine-mediated transfection of D1911 ES cells with two sgRNA expression plasmids targeting *Zfp57* or *Zfp445*, respectively (Table S2). The *Zfp57*$^{-/-}$; *Zfp445*$^{-/-}$ mutant ES clones were obtained by co-transfection of four sgRNA expression plasmids into D1911 ES cells, with two of them targeting *Zfp57* or *Zfp445*, respectively (Table S2). The *Tet* TKO ES clones carrying deletion mutations in the *Zfp57* or *Zfp445* or both genes were generated similarly when the *Tet* TKO ES cells

were used for CRISPR-Cas9 with two sgRNA expression plasmids for each target gene through Lipofect-amine-mediated transfection, with the exception that only one sgRNA plasmid was used for generation of *Zfp57* mutations in the *Tet* TKO ES cells (Table S2).

The *Dnmt1* KO, *Uhrf1* KO and some other mutant ES clones described below were obtained from the parental D1911 ES cells by CRISPR through Lipofectamine-mediated transfection of two sgRNA plasmids each targeting *Dnmt1* or *Uhrf1* or another gene of interest (Tables S3 and S4). An intermediate *Dnmt3b* KO mutant ES clone obtained from the D1911 ES cells by CRISPR was used for Lipofectamine-mediated trans-fection to target *Dnmt3a* in order to obtain the *Dnmt3* DKO mutant ES clones carrying deletion mutations in both *Dnmt3a* and *Dnmt3b* (Table S3). To obtain the *Dnmt* TKO mutant ES clones, an intermediate mutant ES clone with deletion mutations in the *Dnmt1* and *Dnmt3a* genes was first obtained from co-transfections of the sgRNA plasmids into the D1911 ES cells by CRISPR (Table S3). Then this intermediate mutant ES clone was subject to Lipofectamine-mediated transfection of two sgRNA expression plasmids targeting *Dnmt3b* in order to obtain the *Dnmt* TKO mutant ES clones containing deletion mutations in *Dnmt1*, *Dnmt3a* and *Dnmt3b*.

Western blot analysis

Total whole cell lysate samples were obtained from the ES cell culture on a well of 6-well plate. The stan-dard protocol was used for western blot. The blot containing the mutant ES clones for the target gene was subject to immunoblot with the antibodies against the protein product of the target gene. Then the same blot was probed with the antibodies against GAPDH for sample loading assessment.

Immunofluorescence of ES cells

The ES cell culture on 24-well plate was fixed with 4% of paraformaldehyde (PFA) solution for 10 min at 20°C–25°C. Then it was incubated with the antibodies against OCT4 (Santa Cruz Biotechnology, Cat#sc-5279) or NANOG (Santa Cruz Biotechnology, Cat#sc-376915). The fluorescence images were taken under an inverted microscope.

Genomic DNA sample preparation

Genomic DNA samples were harvested from the ES cells after they had been cultured on gelatin-coated plates for one generation to remove almost all feeder cells in ES cell culture. For the genomic DNA samples at Passage 4 (P4) of the control WT, *Dnmt1* KO and *Uhrf1* KO ES clones, they had been cultured on the feeder cells for 4 passages since the parental D1911 ES cells were used for Lipofectamine-mediated trans-fection for isolation of the mutant and control WT ES clones. For the genomic DNA samples at Passage 4 (P4) of *Dnmt3* DKO and *Dnmt* TKO mutant ES clones, they had been cultured on the feeder cells for 4 pas-sages since the last Lipofectamine-mediated transfection for CRISPR-Cas9 in order to obtain the *Dnmt3* DKO and *Dnmt* TKO mutant ES clones from the intermediate $Dnmt3b^{-/-}$ mutant and $Dnmt1^{-/-}$; $Dnmt3a^{-/-}$ mutant ES clones, respectively. The mutant ES clones were used for genomic DNA preparation at P4 soon after they were confirmed to carry deletion mutations at the target genes. Genomic DNA sam-ples at P10 and P20 were obtained from the ES clones after they had been cultured on the feeder cells for a total of 10 and 20 passages, respectively, since the last Lipofectamine transfection of the D1911 ES cells or the intermediate mutant ES cells.

COBRA analysis of the ICRs in ES cells

For COBRA analysis, 1 μg of purified genomic DNA was first subjected to bisulfite treatment with the EZ DNA methylation-Gold™ Kit (Zymo Research #D5006). A fraction of purified bisulfite mutagenized DNA sample was then used for PCR amplification of the ICRs. Usually two rounds of nested PCR reactions were carried out to obtain enough PCR product for restriction enzyme digestion and gel analysis. Then the relative amount of the originally methylated and unmethylated DNA at every tested ICR was estimated based on the band intensities of the digested product on the gels.

Whole-genome bisulfite sequencing (WGBS) of ES samples

Genomic DNA samples for *Dnmt* mutant ES cells and control WT ES cells were harvested from the ES cells devoid of feeder cells after being cultured on gelatin-coated plates for one generation. The purified genomic DNA samples were subjected to whole-genome bisulfite sequencing (WGBS) (Table S5). Low quality sequence reads were removed by Fastp v0.20.0 (https://github.com/OpenGene/fastp). Trim Galore

(v0.4.1, http://www.bioinformatics.babraham.ac.uk/projects/trim_galore/) was applied to trim the adaptor sequences from the raw reads so that the clean reads can be obtained for further analysis. Mapping was carried out for the clean reads by Bismark (v0.13.1; bowtie v2.2.9) (Krueger and Andrews, 2011). Duplicate aligned sequence reads were removed with duplicate_bismark, And Bismark methylation extractor was used to extract the DNA methylation data from the aligned sequence reads after filtering out the duplicate aligned reads. Then DNA methylation of the CpG sites was examined and quantified for all known ICRs as well as somatic DMRs (Table S6). Similar DNA methylation analyses were performed for the repeats and other genomic regions based on the sequence information available on the UCSC website. Please refer to Table S5 for the information regarding the sequenced reads, mapped reads and bisulfite conversion rates of these samples.

Generation of the SNP data for the 129/DBA hybrid ES cells

First, we performed whole-genome sequencing (WGS) for two 129S6/SvEvTac genomic DNA samples. Then the SNPs present in the parental D1911 hybrid ES clone were identified by comparing the 129S6/SvEvTac genomic DNA sequence with that of the DBA2/J genomic DNA sequence in the genome database. Specifically, two genomic DNA samples obtained from the tails of two 129 male mice were subjected to whole genome sequencing (WGS) analysis. The PCR duplicates were removed from the next-generation sequencing (NGS) data before the NGS data were mapped to the genome of DBA/2J mice stored in the UCSC databases using the Burrows-Wheeler Aligner (BWA) tool (v0.7.15-r1140) (Li and Durbin, 2009). Then the Genome Analysis Toolkit (GATK) software package was applied to generate the SNP table with default parameters (McKenna et al., 2010; Van der Auwera et al., 2013).

Assignment of allelic DNA methylation reads

After the SNP data were obtained with BWA and GATK for the parental 129/DBA hybrid ES cell line D1911 mentioned above, all WGBS reads of each ES sample were mapped to the N-masked mouse reference genome that was generated with BEDTools (Quinlan and Hall, 2010). The adaptor sequences were removed using Trim Galore (v0.4.1) as above. The obtained clean reads were further mapped by Bismark (v0.13.1) (Krueger and Andrews, 2011). Then the SNPsplit (v0.3.4) software was used to separate the allelic DNA methylation reads with default parameters (Krueger and Andrews, 2016). The PCR duplicates were removed and DNA methylation at each CpG site was extracted with Bismark (v0.13.1). For each CpG site, only those reads with the SNPs covered more than once were used for further allelic methylation analysis.

QUANTIFICATION AND STATISTICAL ANALYSIS

In WGBS analysis, the percentage of DNA methylation was quantified for each CpG site of an ICR or DMR first with the number of the sequence reads containing methylated C divided by the total number of the sequence reads of this CpG site. Then the average methylation level was calculated for all CpG sites of this ICR or DMR. DNA methylation levels at the repeats, genic regions and whole genome were calculated similarly after the percentage of each CpG site methylation was quantified first and then average methylation level was obtained for all CpG sites afterwards.

Two independent ES clones were obtained for the the *Dnmt1* KO, *Uhrf1* KO, *Dnmt3* DKO, *Dnmt* TKO and the wild-type ES cells. Then their genomic DNA samples were subjected to WGBS analysis thereafter. Statistical analysis was carried out with the R Statistical Software (R version 4.2.1). DNA methylation level at an ICR was compared among the *Dnmt1* KO, *Uhrf1* KO, *Dnmt3* DKO, *Dnmt* TKO and the wild-type ES clones by using one-way or two-way ANOVA with Dunnett multiple comparison test. All statistical analyses are also described in detail in the figure legends as well as in the methods details section. The values in the graphs of the figures were presented as mean $\pm$ SEM with the following statistical significance: $*p < 0.05$; $**p < 0.01$; $***p < 0.001$.